Chemical Geology 276 (2010) 144–165

Contents lists available at ScienceDirect

Chemical Geology

journal homepage: www.elsevier.com/locate/chemgeo

Research papers

Geochronology of the Mesozoic volcanic rocks in the Great Xing'an Range, northeastern China: Implications for subduction-induced delamination

Ji-Heng Zhang [a,*], Shan Gao [b], Wen-Chun Ge [c], Fu-Yuan Wu [a], Jin-Hui Yang [a], Simon A. Wilde [d], Ming Li [b]

[a] State Key Laboratory of Lithospheric Evolution, Institute of Geology and Geophysics, Chinese Academy of Sciences, P.O. Box 9825, Beijing 100029, China
[b] State Key Laboratory of Geological Processes and Mineral Resources, School of Earth Sciences, China University of Geosciences, Wuhan 430074, China
[c] College of Earth Sciences, Jilin University, Changchun 130061, China
[d] Department of Applied Geology, Curtin University of Technology, P O Box U1987, Perth, Western Australia 6845, Australia

ARTICLE INFO

Article history:
Received 11 December 2009
Received in revised form 12 May 2010
Accepted 14 May 2010

Editor: R.L. Rudnick

Keywords:
Zircon U–Pb and ^{40}Ar–^{39}Ar geochronology
Mesozoic volcanic rocks
Great Xing'an Range
Delamination
Northeastern China

ABSTRACT

Mesozoic volcanic rocks and granitoids are widespread in the Great Xing'an Range, which is part of a large igneous province in the eastern China. However, the ages of the volcanic rocks, especially those in the southern segment of the range, are poorly constrained. Here we present zircon U–Pb and whole rock Ar–Ar ages of 43 volcanic rocks from the four recognized formations (Manketouebo, Manitu, Baiyingaolao and Meiletu) in the southern Great Xing'an Range. The volcanic rocks of the Manketouebo Formation have a large span of ages ranging from 174 to 122 Ma, while those of the Manitu Formation exhibit a smaller age range from 156 to 125 Ma. The Baiyingaolao and Meiletu volcanic rocks both have Early Cretaceous ages between 139 and 124 Ma. These data indicate that the mapped units are not strictly 'formations' and further studies are required to resolve this issue. However, when taken together, these new data define two episodes of magmatism (Late Jurassic and Early Cretaceous) with the Early Cretaceous volcanic rocks being dominant. Combined with previously published data from the northern Great Xing'an Range, and available age data from other parts of northeastern China and surrounding regions, two stages of magmatism, i.e., Jurassic and Early Cretaceous, can be identified throughout this part of Asia. The Jurassic rocks mainly comprise granites, while volcanic rocks are dominant in the Early Cretaceous. These two stages of magmatism form opposite spatial trends, that is, the Jurassic rocks become younger to the west, whereas the Cretaceous rocks become younger to the east. Between the two stages of magmatism, the 'magma gap' increases eastward in duration from less than 10 Ma in the Great Xing'an Range to more than 40 Ma in Japan. These trends can be explained by westward subduction of the Paleo-Pacific oceanic Plate and its control on subsequent geodynamic processes. Jurassic subduction of the oceanic slab caused crustal shortening and thickening, and formed the westward decrease in age of the granites with characteristics of an active continental margin, while volcanism was rare. By the end of the Jurassic, westward flat-slab subduction of the Paleo-Pacific Oceanic plate changed its direction to the north or northwest. This subsequently caused a transformation in tectonic regime from compression to extension in the Cretaceous and induced large-scale delamination of the thickened lower crust and lithospheric mantle. Delamination was initiated at the western margin of the subducting slab, and migrated eastward. Delamination and consequent upwelling of the asthenosphere triggered extensive volcanic eruption, with only minor granite emplacement. Similar age trends are also observed for other parts of eastern China, suggesting this model can also be applied to explain the geodynamic setting of the Mesozoic large igneous events in China and adjacent regions.

1. Introduction

Delamination is a process whereby the lithospheric mantle, lower continental crust and/or oceanic crust sink into the asthenosphere, driven by gravitational instability (e.g., Bird, 1979; Lustrino, 2005), resulting in the upwelling of the asthenosphere to the base of the crust, which dramatically changes the structure and composition of the mantle–crust system. It is commonly accompanied by crustal uplift, basin formation and voluminous magmatism (e.g., Kay and Kay, 1993). Taking eastern China as an example, delamination is considered to be an important mechanism to explain lithospheric thinning, voluminous Mesozoic magmatism and the evolved composition and slow seismic velocities of the crust (Gao et al., 1998a,b; Wu and Sun, 1999; Wu et al., 2000c; Gao et al., 2002; Wu et al., 2003a,c; Gao et al., 2004; Wu et al., 2005a, 2006; Deng et al., 2006, 2007), although several other models have been proposed, such as thermal

* Corresponding author. Tel.: +86 10 82998445; fax: +86 10 62010846.
E-mail address: zhangjh@mail.igcas.ac.cn (J.-H. Zhang).

0009-2541/$ – see front matter
doi:10.1016/j.chemgeo.2010.05.013

erosion (Menzies and Xu, 1998; Griffin et al., 1998; Zheng et al., 1998; Zheng et al., 2001; Xu, 2001; Xu et al., 2004; Zheng et al., 2006, 2007; Xu et al., 2008a) and peridotite-melt reaction (Zhang et al., 2002a; Zhang, 2005; Zhang et al., 2007a). However, the controlling tectonic factors, timing and scenario of delamination are essentially unknown and it has been attributed to several different events, including as the result of accretion of the North China Craton (NCC) with the Yangtze Craton (YC) (Menzies and Xu, 1998; Gao et al., 2002, 2004; Xu et al., 2006, 2008b), or by the subduction of the Paleo-Pacific plate during the late Mesozoic (Wu and Sun, 1999; Wu et al., 2000c, 2003a; Wang et al., 2006b; Zhang et al., 2008b). An examination of the voluminous magmatic rocks in eastern China could provide a useful way to resolve this issue. Compilations of the available age data for the huge igneous belt in eastern China have shown that the rocks mostly formed in the Early Cretaceous with a peak at 125 Ma; and this was considered to relate to delamination and the induced lithospheric thinning (Wu et al., 2005a). On the other hand, the Jurassic is also an important epoch for igneous activity in eastern China, and along the eastern Asian continental margin in general (Wu et al., 2005b). However, the petrogenesis and tectonic affinity of these rocks remain controversial, especially the relationship between magmatism and subduction of the Paleo-Pacific plate, which may be better resolved by studies of Mesozoic magmatism in eastern China, including the Great Xing'an Range (Fig. 1a), for which the age frame is largely unknown.

Mesozoic volcanic rocks are dominant in the Great Xing'an Range and adjacent areas of northeastern (NE) China, and constitute one of the most striking geological features along the eastern Asian continental margin. The Great Xing'an Range corresponds to not only a sharp gravity anomaly and east–west topographic boundary, but also a boundary that penetrates the lithosphere (e.g., Xu, 2006). Recent geochronological studies indicate the volcanic rocks in the northern Great Xing'an Range were mainly erupted in the Early Cretaceous (Wang et al., 2006b; Zhang et al., 2008b and references therein). The published ages of the volcanic rocks indicate that the previous subdivision and time assignment of the volcanic strata are questionable and need to be re-evaluated. However, the geochronological framework of the volcanic rocks in the southern Great Xing'an Range is still unclear due to the lack of precise age data, since only a few zircon U–Pb and whole rock Ar–Ar ages from restricted regions have been reported (Zhang, 2006; Chen et al., 2007; Guo et al., 2008). The important remaining question is whether the volcanic rocks in the southern Great Xing'an Range have a similar age range to those of the northern segment.

This paper presents the results of the first systematic dating of the volcanic rocks from the southern Great Xing'an Range. A total of forty-three samples, including rhyolite/felsite, rhyolitic tuff/ignimbrite, dacite, and andesite from all the four named formations were dated by the single zircon U–Pb method and whole rock $^{40}Ar/^{39}Ar$ incremental technique. The age data provide essential constraints on the timing, subdivision, and regional correlation of the volcanic strata. The geochronological data are then combined with the age data from adjacent regions to evaluate the evolution of magmatism in northeastern, and further eastern China.

2. Geological setting

Eastern China comprises the Xing'an–Mongolian Orogenic Belt (XMOB) and part of the North China Craton (NCC) in the north, the Qinling–Dabie–Sulu Ultra-High Pressure metamorphism belt and Yangtze Craton (YC) in the central part, and the SE China Orogenic Belt (SECOB) in the south. One striking feature of eastern China is the occurrence of large volumes of Mesozoic igneous rocks along the continental margin (Meng, 2003; Wu et al., 2005a,b; Fig. 1a). Most of these igneous rocks formed in the Jurassic–Early Cretaceous (Yanshanian) and comprise two separate episodes. The most significant period of magmatism in the Jurassic is between 195 and 150 Ma, whereas the igneous rocks of Early Cretaceous age have a much shorter duration, with the most important period being between 130 and 120 Ma, with the peak at ~125 Ma (Wu et al., 2005a,b and references therein).

The XMOB is considered to be the eastern part of the Paleozoic Central Asian Orogenic Belt (CAOB), located between the Siberian and North China cratons (Sengör et al., 1993; Jahn et al., 2000; Jahn, 2004; Li, 2006b). It is composed of a series of micro-continents (Ye et al., 1994), separated from the North China Craton by the Chifeng–Kaiyuan fault belt in the south, and comprising the Erguna and Xing'an blocks in the northwest, the Songliao Block in the central part and the Jiamusi Massif in the east, separated by the Tayuan–Xiguitu, Hegenshan–Hehei and Jiayin–Mudanjiang faults, respectively (Wu et al., 2007a; Fig. 1b). Due to the dense vegetation cover, the geological features of the Erguna Block are poorly known, although recent studies indicate that Paleozoic granitoids are well developed (Ge et al., 2005a; Wu et al., 2005c; Ge et al., 2007a). Geochronological studies also show that the metamorphic basement rocks are Neoproterozoic to Cambrian in age (Miao et al., 2007) and not Paleoproterozoic as previously thought (IMBGMR, 1991; HBGMR, 1993).

The Xing'an Block is mostly located in the Great Xing'an Range, and is characterized by voluminous Mesozoic granite and volcanic rocks (Fan et al., 2003; Ge et al., 2005b; Zhang et al., 2006a,b; Wang et al., 2006b; Ge et al., 2007b; Sui et al., 2007; Zhang et al., 2008b). Previously identified Proterozoic metamorphic rocks (IMBGMR, 1991) are now considered to be Paleozoic in age on the basis of recent geochronological studies (Miao et al., 2004, 2007). The Songliao Block is largely covered by the Songliao sedimentary basin. Recent studies indicate that Early Cretaceous volcanic rocks underlie a large proportion of the basin (Wang et al., 2002; Zhang et al., 2007b; Shu et al., 2007; Ding et al., 2007; Gao, 2008). Borehole drill core also reveals that granites are widespread in the basement, with some Precambrian components (Wu et al., 2000b, 2001; Wang et al., 2006a; Pei et al., 2007; Gao et al., 2007; Wang and Wang, 2007; Xu et al., 2008c; Zhang et al., 2008a). To the northeast and east, Mesozoic volcanic rocks and granites are dominant in the Lesser Xing'an and Zhangguangcai Ranges with rare remnants of Paleozoic strata sporadically dispersed in these igneous rocks (Wu et al., 2000a). The Jiamusi Massif contains three different rock series: the Mashan complex, the Heilongjiang complex and Early and Late Paleozoic granitoids. The Mashan complex is characterized by khondalitic rocks (aluminous paragneiss, marble, and graphitic schist), metamorphosed to granulite facies. It was traditionally considered to be Late Archean in age (HBGMR, 1993), but recent studies showed that metamorphism took place at *ca* 500 Ma (Wilde et al., 1997, 2000). Two ages of granitoids have been identified: deformed and metamorphosed granitoids of Late Pan-African age (*ca* 520 Ma; Wilde et al., 2003), and weakly to un-deformed Permian granites with ages of *ca* 260 Ma (Wilde et al., 1997; Wu et al., 2000a). The rock association and field relationship of the Heilongjiang complex indicate tectonic juxtaposition, and it represents a mélange along the Asian continental margin accreted during the Early Jurassic. Based on recent geochronological investigations, it is concluded that the Jiamusi Massif is an exotic terrane amalgamated to the east margin of the Asian continent in the Jurassic (Wu et al., 2007a; Zhou et al., 2009).

During the Phanerozoic, NE China underwent a complex history, highlighted by multiple stages of accretion and collision (Sengör et al., 1993), although the time and manner of the amalgamation of the micro-continents still remains controversial. It has been proposed that the Erguna Block collided with the Xing'an Block during the Early Paleozoic, based on studies of ophiolitic complexes along the Tayuan–Xiguitu Fault and the presence of Early Ordovician post-orogenic granites (Yan et al., 1989; Zhang and Tang, 1989; Li, 1991; Ge et al., 2005a). The Songliao Block was then accreted to the Xing'an–Erguna composite block along the Hegenshan–Heihe suture in the Late Devonian to Early Carboniferous (Ye et al., 1994; Hong et al., 1994;

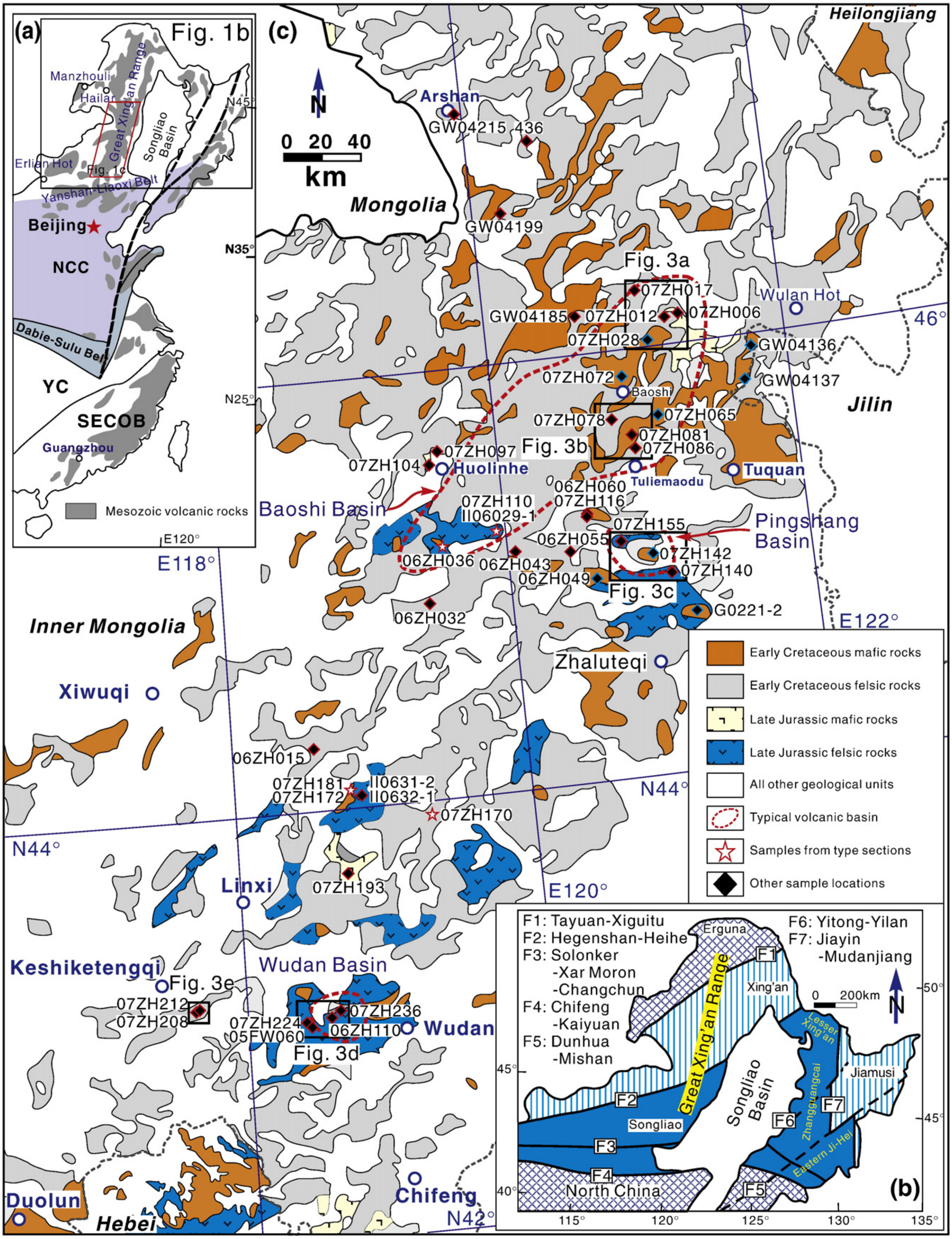

Fig. 1. (a) Simplified tectonic units of eastern China showing the distribution of the Mesozoic volcanic rocks (Meng, 2003; and Wu et al., 2005a). XMOB: Xing'an–Mongolian Orogenic Belt; NCC: North China Craton; YC: Yangtze Craton; SECOB: SE China Orogenic Belt. (b) Tectonic subdivisions of northeastern China (after Wu et al., 2007a). (c) Distribution of Mesozoic volcanic rocks in the southern Great Xing'an Range, showing sample locations (based on HBGMR, 1989; IMBGMR, 1991; HBGMR, 1993).

Robinson et al., 1999; Chen et al., 2000; Sun et al., 2001a; Wu et al., 2002; Shi et al., 2004; Zhou et al., 2005). Subsequently, regional extension developed in the late Paleozoic (Tang, 1990). Nd and Hf isotopic studies on the granitoids indicate that NE China underwent significant crustal growth during both the Meso- to Neoproterozoic and the Phanerozoic (Jahn et al., 2000; Wu et al., 2000b, 2002, 2003b; Ge et al., 2007a; Sui et al., 2007), which is also evident from isotopic studies of volcanic rocks (Zhang et al., 2006a, 2007a; Fan et al., 2008; Guo et al., 2008).

3. Mesozoic volcanic rocks in the southern Great Xing'an Range

According to Zhao et al. (1989), the southern Great Xing'an Range extends from N47°20′ in Inner Mongolia to the north of Weichang County (N42°) in Hebei Province, located mainly in the western part of the Songliao Block and including the northern margin of the NCC (Fig. 1). This study is restricted to the region north of the Chifeng–Kaiyuan fault belt, marking the boundary between the XMOB and NCC.

The volcanic rocks in the southern Great Xing'an Range are mainly distributed in several discrete basins, including the Baoshi, Pingshan and Wudan basins (refer to Fig. 1c), and have been subdivided into the Manketouebo, Manitu, Baiyingaolao and Meiletu formations in Inner Mongolia (Zhao et al., 1989; IMBGMR, 1991; Wang et al., 1997), and this is commonly accepted in the Chinese literature (Fig. 2b). These volcanic rocks unconformably overlie the coal-bearing strata of the Wanbao/Xinmin Formation, which is considered to be of Middle Jurassic age, and hence the volcanic rocks were considered to be Late Jurassic in age. It is notable that the Xinmin Formation also contains some tuffaceous interlayers, with volcanoclastic rocks locally dominant.

The basal Manketouebo Formation was first defined at the southwestern margin of the Baoshi Basin (Fig. 1c). According to the original definition, at this locality it unconformably overlies Permian strata and is widespread across the whole region. It comprises a suite of felsic lavas, tuffs, ignimbrites and volcanoclastic rocks of variable thickness, intercalated with some mafic volcanic and sedimentary rocks. Lithologically, most of the rocks are porphyritic, with phenocrysts of plagioclase, K-feldspar, sanidine and quartz set in a felsitic matrix; some dark rimmed biotite and hornblende crystals also occur as phenocrysts. Alteration of the plagioclase and the K-feldspar is common, while embayed euhedral quartz is also ubiquitous.

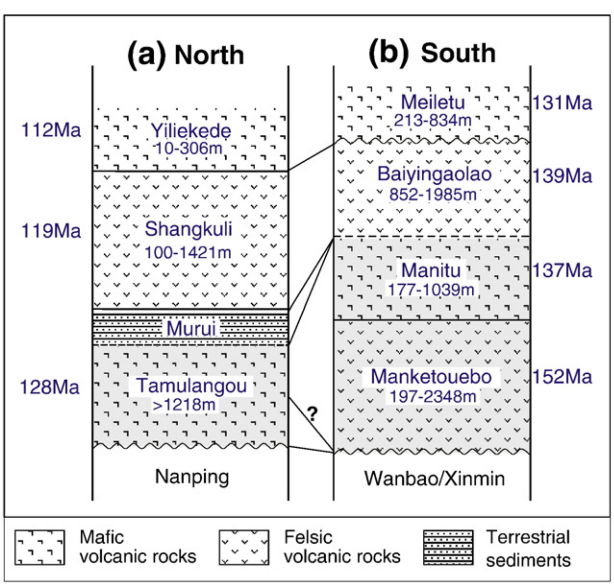

Fig. 2. Stratigraphic subdivisions of the Mesozoic volcanic rocks in the Great Xing'an Range: (a) the northern segment; (b) the southern segment (based on IMBGMR, 1991; HBGMR, 1993; Wang et al., 1997). The marked thicknesses were obtained from outcrops at different locations. The marked ages are those obtained from the type sections of these formations, which suggest that at least some of the sequence is incorrect.

The Manitu Formation was defined as a suite of intermediate (andesitic) volcanic rocks overlying the Manketouebo Formation. It is mostly restricted to the margin of the basin and everywhere overlies the Manketouebo Formation, although it is less widely distributed. It is composed by a series of intermediate volcanic and related volcanoclastic rocks of variable thickness, intercalated with local dacite and felsic tuffaceous rocks. The rocks are commonly porphyritic with phenocrysts of plagioclase, pyroxene, biotite, and hornblende dispersed in a fine-grained or vitreous matrix. Alteration of the plagioclase is commonly observed, whereas, hornblende and biotite are commonly rimmed by opaque oxides.

According to the original definition, the Baiyingaolao Formation comprises felsic volcanoclastic rocks and sediments, which overlie the Manitu Formation. It is everywhere associated with the Manketouebo Formation, but is mainly restricted to the northern part of the area. Lithologically, it is similar to the Manketouebo Formation, but with a larger percentage of aphanitic rocks without phenocrysts and voluminous volcanoclastic rocks. The outcrop thickness varies considerably between basins.

The Meiletu Formation forms the upper part of the volcanic sequence, representing the final phase volcanism in the region. It is defined as a suite of intermediate-mafic volcanic rocks unconformably overlying felsic rocks of the Baiyingaolao Formation and older strata. It is mainly distributed in the center of the various volcanic basins. The rocks comprise basalt, pyroxene-bearing basaltic andesite, pyroxene andesite, biotite andesite, and related volcanoclastic rocks and columnar structures are common. Most rocks are fresh and have a porphyritic texture, with phenocrysts of plagioclase, pyroxene, hornblende, biotite, and minor olivine, set in a fine-grained groundmass or brown glass.

Several general features are evident for the volcanic rocks in the study area, as follows:

(1) The volcanic rocks in the southern Great Xing'an Range are dominated by felsic and related volcanoclastic rocks, with only minor mafic-intermediate rocks. The thickness of these volcanic rocks varies from several hundred to several thousand meters. The intermediate-mafic rocks comprise andesites, basaltic andesites, and rare trachy-andesites and are mainly distributed in several intracontinental basins, including the Baoshi Basin in the north, the Pingshan Basin to the east and the Wudan Basin in the south (Fig. 1c; Zhao et al., 1989). The Baoshi Basin is the largest and contains thick sequences of all four formations. The Hatumohe section at the northern margin and the Tuliemaodu section in the southeast (Fig. 3a and b, respectively) are typical sections. In the center of the southern Great Xing'an Range, the Chaganbulage section in the Pingshan Basin also contains all four formations and forms a syncline with the Meiletu Formation in the center (Fig. 3c). In the Wudan basin, the Paotai section comprises the Manketouebo, Manitu and Baiyingaolao Formations (Fig. 3d). To the southeast of Keshiketengqi in the southern part of the area, volcanic rocks of the Manketouebo, Manitu and Baiyingaolao Formations are present with the Baiyingaolao Formation in the center (Fig. 3e). In order to constrain the timing of volcanism, volcanic sequences within these basins provide the key sections for this study.

(2) The regional correlation of the volcanic strata between the northern and southern segments of the Great Xing'an Range is imprecise. It was traditionally considered that the onset of volcanism was earlier in the northern segment than in the south (Zhao et al., 1989; IMBGMR, 1991; Wang et al., 1997). The Manketouebo Formation in the southern segment is

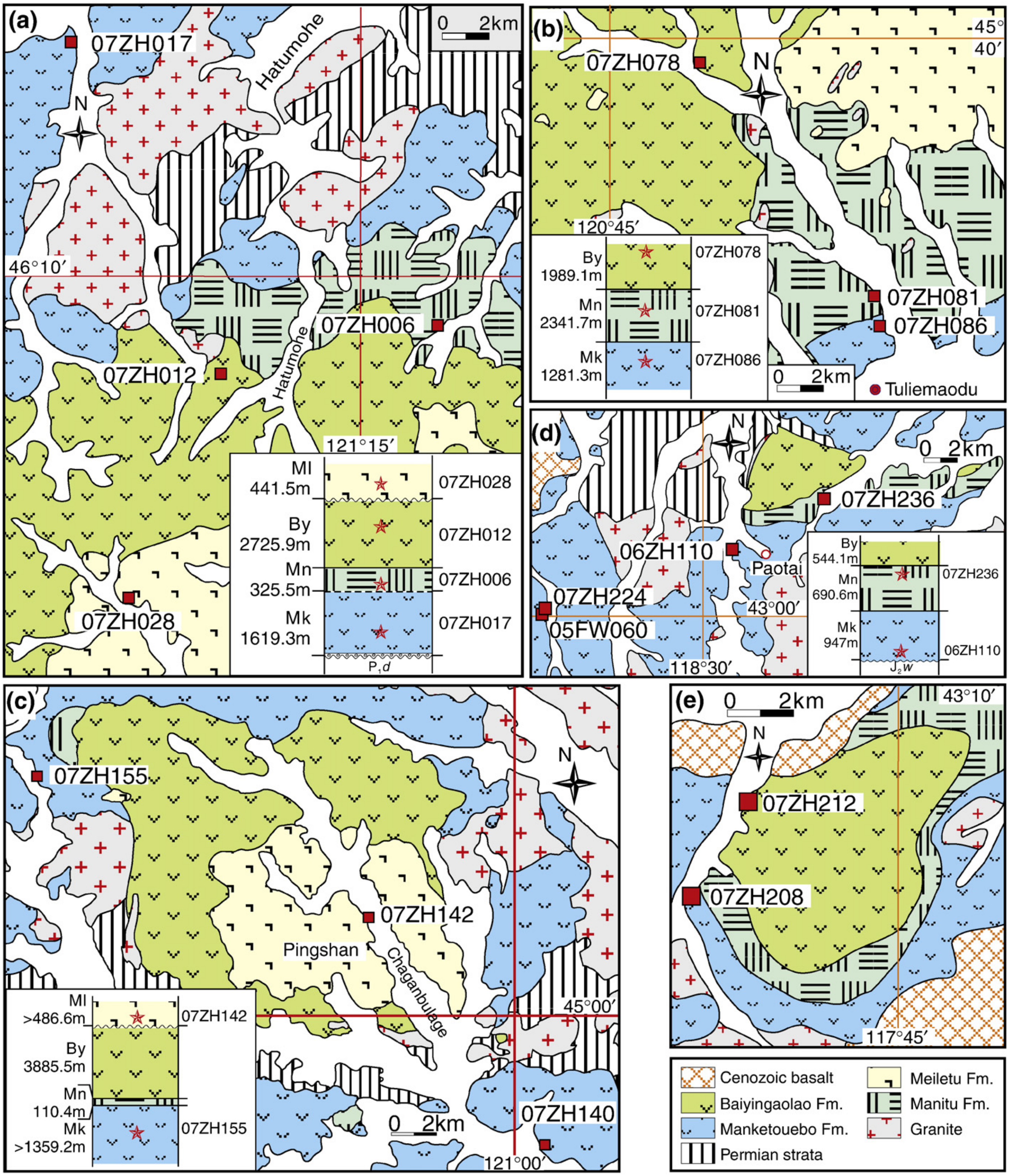

Fig. 3. Simplified geological maps of selected areas in the southern Great Xing'an Range showing stratigraphic sections and sample locations. (a) The Hatumohe section in the north of the Baoshi Basin; (b) the Tuliemaodu section from the southeastern Baoshi Basin; (c) the Chaganbulage section in the Pingshan Basin; (d) the Paotai section in the northern part of the Wudan Basin; and (e) the Keshiketengqi section in the southern part of the southern Great Xing'an Range. Mk: Manketouebo Formation; Mn: Manitu Formation; By: Baiyingaolao Formation; Ml: Meiletu Formation.

correlated with the upper section of the Tamulangou Formation in the northern segment (Fig. 2). But recent geochronological studies do not support this proposal (Wang et al., 2006b; Zhang et al., 2008b; see later discussion).

(3) The Manketouebo and Baiyingaolao formations have similar rock assemblages and geochemistry, although some rocks of the Manketouebo are less alkaline (refer to Fig. 4b), and the formations were mainly differentiated in the field by the

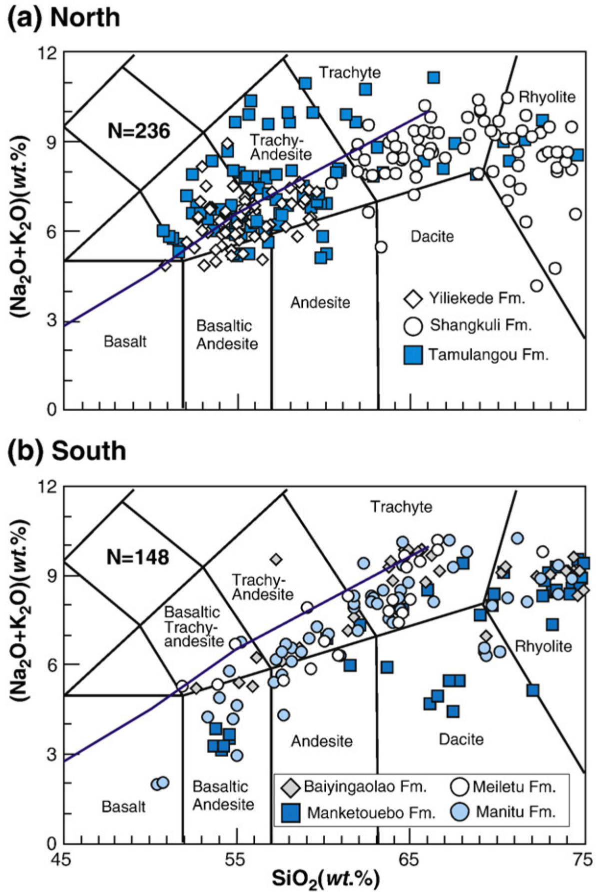

Fig. 4. TAS classification diagrams of the volcanic rocks from the Great Xing'an Range: (a) rocks from the northern segment (Zhang et al., 2008b); and (b) rocks from the southern segment (Zhao et al., 1989; Ge et al., 1999, 2000a; Guo et al., 2001; Gao et al., 2005; Lin et al., 2003).

presence of intermediate rocks in the Manitu Formation. Felsic rocks were thus considered to belong to the Manketouebo Formation when they were overlain by the intermediate rocks of the Manitu Formation; in contrast, when they were above intermediate rocks, they were classified as Baiyingaolao Formation. However, classification is commonly impossible in the field, especially at locations where the stratigraphic section is limited as a result of either tectonic disruption or vegetation cover. In addition, the Manketouebo and Baiyingaolao Formations also contain some intercalated intermediate-mafic rocks, which further confuses the discrimination of the two felsic formations.

(4) Geochemically, the volcanic rocks cover a wide range of rock types, including basaltic trachy-andesites, trachy-andesites, trachytes and rhyolites, with few basalts, and dacites (Fig. 4b; Zhao et al., 1989; Ge et al., 1999; Guo et al., 2001; Lin et al., 2004; Gao et al., 2005; Guo et al., 2008; Zhang et al., 2008c; and unpublished data). The rocks are mainly sub-alkaline (Irvine and Baragar, 1971), which is different from the northern segment (Zhang et al., 2008b and references therein), where many rocks are richer in alkalis (Fig. 4). In the TAS diagram, it is evident that volcanic rocks from the different formations show the same geochemical trends and are largely indistinguishable, although the Manketouebo Formation rocks tend to have lower total alkalis (Fig. 4). The mafic-intermediate rocks are chemically quite variable, indicating heterogeneous magma sources and different petrogeneses (Ge et al., 1999, 2000b; Guo et al., 2001; Fan et al., 2003; Lin et al., 2003; Gao et al., 2005; Chen et al., 2006; Zhang et al., 2006a,b, 2007a, 2008c). The felsic rocks also show a wide range of trace and rare earth (REE) element patterns. The most striking feature is the variation in Ba–Sr abundances (Ge et al., 2000a; Lin et al., 2000, 2003), revealing complexities in the magma sources. Geochemical studies also indicate the existence of adakitic volcanic rocks in the southern segment (Gao et al., 2005).

There is almost a complete absence of precise age data for the volcanic rocks in the southern Great Xing'an Range, with only a few data reported. For example, Guo et al. (2008) reported an Early Cretaceous age for a dacite in the Huolinhe region, in the northwestern segment of the southern Great Xing'an Range, whereas volcanic rocks in the Erlian Basin, to the west of the Great Xing'an Range were also reported to be Early Cretaceous (Chen et al., 2007). But these ages are inadequate to define the volcanism. In the present work, a total of forty-three samples were dated by the zircon U–Pb method and by the whole rock $^{40}Ar/^{39}Ar$ incremental technique. These samples were collected not only from the type sections of each formation, but also from additional sections within several of the basins (refer to Fig. 3) in order to precisely characterize volcanism in the southern Great Xing'an Range. Brief descriptions of the samples are given in Table 1.

4. Analytical methods

A total of 41 samples were dated by LA-ICPMS, one by TIMS, and one by the $^{40}Ar/^{39}Ar$ incremental heating method. The laser ablation inductively-coupled mass spectrometry (LA-ICPMS) method now has an accuracy comparable to that of secondary-ion mass spectrometry (SIMS) for Phanerozoic zircons (Horn et al., 2000; Li et al., 2000; Ballard et al., 2001; Li et al., 2001; Košler et al., 2002; Yuan et al., 2003; Jackson et al., 2004; Yuan et al., 2004; Paul et al., 2005; Liu et al., 2007), with mass discrimination and isotopic fractionation during ablation and transportation greatly improved by external correction using standard zircons (Black et al., 2004). Pristine zircons were selected and mounted in resin and polished to approximately half their thickness. They were then imaged in cathodoluminescence (CL) using a Mono CL3+ (Gatan Company, England) at the State Key Laboratory of Continental Dynamics, Department of Geology, Northwest University, Xi'an. Zircon LA-ICPMS dating was completed both in the State Key Laboratory of Continental Dynamics, Northwest University in Xi'an and the State Key Laboratory of Geological Processes and Mineral Resources, China University of Geosciences, Wuhan. The two laboratories have the same equipment for laser ablation (GeoLas200M) and inductivity coupled plasma mass spectrometry (Agilent 7500a). During analysis, the synthetic glass NIST 610 was used to optimize the instruments, and the standard zircon 91500 was used as an external standard to monitor the status of the machines. The detailed instrumental parameters and the protocol of analyses follow Yuan et al. (2004, 2008), Liu et al. (2010) and Liu et al. (2007). The raw data were then processed using the Glitter (Version 4.0) program of Macquarie University, and the common lead was corrected following the method of Andersen (2003) The weighted mean age was calculated using Isoplot (Version 3.23) (Ludwig, 2003). Analyses with >10% discordance are excluded from the calculations. The isotopic ratios and age are quoted at 1σ, whilst, the weighted mean is given at the 95% confidence level (Supplementary Table 1).

A rhyolite (sample 436) from the Baiyingaolao Formation was dated using thermal ionization mass spectrometry (TIMS) at the Tianjin Institute of Geology and Mineral Resources, Chinese Academy of Geological Sciences. The analytical protocol followed Li et al. (1995). A ^{205}Pb–^{235}U spike was added to the zircon samples in a 0.25 mL Teflon capsule for dissolution. The final isolated U and Pb were loaded onto a Re filament with silica gel-phosphoric acid. All U and Pb data were corrected for mass fractionation. The blanks were

Table 1
Sample locations of the dated volcanic rocks in the southern Great Xing'an Range.

Sample no.	Location	Latitude and longitude	Formation	Rock type	Method	Age (Ma)
05FW060	Maoshandong	43°00′31″N 118°24′03″E	Manketouebo	Rhyolite	LA-ICP-MS	174 ± 4
06ZH032	Baritu	44°53′11″N 119°23′40″E	Manketouebo	Rhyolite	LA-ICP-MS	133 ± 2
06ZH110	Paotai	43°02′23″N 118°21′04″E	Manketouebo	Rhyolite	LA-ICP-MS	154 ± 1
07ZH097	Huolinhe	45°36′08″N 119°33′11″E	Manketouebo	Rhyolite	LA-ICP-MS	150 ± 2
07ZH110	Manketouebo	45°14′08″N 119°53′53″E	Manketouebo	Rhyolite	LA-ICP-MS	156 ± 1
II06029-1	Manketouebo	45°13′56″N 119°54′45″E	Manketouebo	Rhyolite	LA-ICP-MS	153 ± 8
07ZH172	Manitu	44°04′54″N 118°45′50″E	Manketouebo	Rhyolite	LA-ICP-MS	163 ± 1
II06031-2	Manitu	44°05′36″N 118°47′29″E	Manketouebo	Rhyolite	LA-ICP-MS	160 ± 2
II06032-1	Manitu	44°05′36″N 118°47′29″E	Manketouebo	Rhyolite	LA-ICP-MS	165 ± 1
07ZH017	Alider	46°15′16″N 121°05′34″E	Manketouebo	Dacite	LA-ICP-MS	138 ± 1
07ZH155	Sebuer	45°05′45″N 120°44′11″E	Manketouebo	Dacite	LA-ICP-MS	151 ± 1
GW04199	Sancha	46°39′40″N 120°08′27″E	Manketouebo	Dacite	LA-ICP-MS	124 ± 2
07ZH104	Huolinhe	45°32′44″N 119°31′45″E	Manketouebo	Andesite	LA-ICP-MS	157±2
07ZH140	Gahaitu	44°56′36″N 121°01′30″E	Manketouebo	Andesite	LA-ICP-MS	150 ± 3
07ZH086	Tuliemaodu	45°33′26″N 120°53′45″E	Manketouebo	Rhyolitic tuff	LA-ICP-MS	128 ± 1
07ZH208	Shanghuofang	43°06′34″N 117°40′35″E	Manketouebo	Ignimbrite	LA-ICP-MS	135 ± 2
07ZH224	Tuchengzi	43°01′00″N 118°22′52″E	Manketouebo	Ignimbrite	LA-ICP-MS	153 ± 2
07ZH006	Baoantun	46°08′52″N 121°17′31″E	Manitu	Andesite	LA-ICP-MS	151 ± 2
07ZH181	Manitu	44°04′59″N 118°45′37″E	Manitu	Andesite	LA-ICP-MS	138 ± 1
06ZH049	Balimuhade	44°55′26″N 120°32′43″E	Manitu	Andesite	LA-ICP-MS	132 ± 1
G0221-2	Keyouzhongqi	44°59′27″N 121°17′02″E	Manitu	Hornblende andesite	LA-ICP-MS	129 ± 2
GW04136	Eti	45°55′44″N 121°46′40″E	Manitu	Pyroxene-andesite	LA-ICP-MS	125 ± 1
GW04137	Naoniushan	45°47′16″N 121°40′36″E	Manitu	Pyroxene-andesite	Ar–Ar	128.6 ± 3.1
07ZH236	Paotai	43°04′03″N 118°36′02″E	Manitu	Dacite	LA-ICP-MS	156 ± 1
07ZH193	Wulahai	43°41′07″N 118°42′43″E	Manitu	Rhyolite	LA-ICP-MS	155 ± 1
07ZH081	Herimu	45°34′15″N 120°53′18″E	Manitu	Rhyolitic tuff	LA-ICP-MS	126 ± 1
436	Arshan	–	Baiyingaolao	Rhyolite	TIMS	125.9 ± 1.2
GW04185	Sharentai	46°21′18″N 120°34′21″E	Baiyingaolao	Rhyolite	LA-ICP-MS	135 ± 1
GW04215	Arshan	47°09′07″N 119°56′33″E	Baiyingaolao	Rhyolite	LA-ICP-MS	124 ± 1
06ZH015	Huitonghe	44°16′44″N 118°35′29″E	Baiyingaolao	Rhyolite	LA-ICP-MS	131 ± 1
06ZH043	Aletandaban	45°07′32″N 120°01′08″E	Baiyingaolao	Rhyolite	LA-ICP-MS	129 ± 1
06ZH055	Bayartuhushuo	45°05′32″N 120°22′38″E	Baiyingaolao	Felsite	LA-ICP-MS	132 ± 1
07ZH078	Wulanhade	45°39′20″N 120°47′39″E	Baiyingaolao	Dacite	LA-ICP-MS	131 ± 1
07ZH012	Zhongxintun	46°07′56″N 121°10′23″E	Baiyingaolao	Ignimbrite	LA-ICP-MS	137 ± 1
07ZH170	Baiyingaolao	43°55′59″N 119°17′41″E	Baiyingaolao	Ignimbrite	LA-ICP-MS	138 ± 1
07ZH212	Shanghuofang	43°07′54″N 117°41′37″E	Baiyingaolao	Ignimbrite	LA-ICP-MS	139 ± 2
07ZH028	Baoshi	46°02′44″N 121°07′21″E	Meiletu	Andesite	LA-ICP-MS	128 ± 9
07ZH142	Chaganbulage	45°02′23″N 120°55′22″E	Meiletu	Andesite	LA-ICP-MS	128 ± 1
07ZH072	Zhangjiajie	45°52′09″N 120°52′42″E	Meiletu	Hornblende andesite	LA-ICP-MS	128 ± 2
07ZH116	Wulanhada	45°17′05″N 120°34′37″E	Meiletu	Hornblende andesite	LA-ICP-MS	134 ± 2
06ZH036	Meiletu	45°12′54″N 119°32′42″E	Meiletu	Pyroxene-andesite	LA-ICP-MS	131 ± 1
06ZH060	Wulanhada	45°15′39″N 120°34′23″E	Meiletu	Biotite-andesite	LA-ICP-MS	128 ± 1
07ZH065	Jiefangtun	45°38′23″N 121°10′50″E	Meiletu	Basaltic andesite	LA-ICP-MS	126 ± 4

0.05 ng for Pb and 0.002 ng for U. The obtained isotopic ratios and the age data are reported at the 2σ level (Table 2).

The groundmass of one basaltic andesite from the Manitu Formation was dated by the $^{40}Ar/^{39}Ar$ incremental heating technique, since no zircon was present in the rock. The $^{40}Ar/^{39}Ar$ dating was performed at the Geochronology Laboratory in the Institute of Geology and Geophysics, Chinese Academy of Sciences, Beijing; the analytical protocol follows Wang et al. (2005). The sample wafer, together with neutron fluence monitor mineral, were irradiated *in vacuo* within a cadmium-coated quartz vial for 45.8 h in position H8 at the Beijing Atomic Energy Research Institute reactor (49–2). The neutron flux gradient was determined to be within ± 0.7% by repeated analyses of the monitor mineral, and this uncertainty is propagated into the plateau and isochron ages. Interfering nucleogenic reactions were checked by using CaF_2 and K_2SO_4; while the mass discrimination was monitored by an online air pipette, from which multiple measurements before and after each heating step were taken. Irradiated samples were then placed into a Ta tube resting in the Ta crucible of an automated double-vacuum resistance furnace and incrementally heated in 14 steps at 10 min intervals from 780 C to 1450 C. Following 5 additional minutes of gas purification on Al–Zr getters, isotopic measurements were performed on a MM5400 mass spectrometry with a Faraday cup and an electron multiplier. The hot system blanks, which were determined several times each day prior to

Table 2
Zircon TIMS U–Pb data for sample 436.

Zircon features			Concentration			Common lead (ng)	Isotopic ratios								Apparent age (Ma)		
Analysis no.		Color	Wt. (mg)	U (mg/g)	Pb (mg/g)		$^{206}Pb/^{204}Pb$	$^{208}Pb/^{206}Pb$	$^{206}Pb/^{238}U$	2σ	$^{207}Pb/^{235}U$	2σ	$^{207}Pb/^{206}Pb$	2σ	$^{206}Pb/^{238}U$	$^{207}Pb/^{235}U$	$^{207}Pb/^{206}Pb$
436	1	Light yellow	15	1798	62	0.320	124	0.3023	0.01967	23	0.1318	26	0.04859	72	125.6	125.7	128.0
(Baiyingaolao	2	Light yellow	10	1478	45	0.100	199	0.3631	0.01956	45	0.1313	48	0.04870	128	124.9	125.3	133.3
Formation)	3	Light purple–red	15	980	33	0.160	137	0.2737	0.02001	43	0.1342	49	0.04864	130	127.7	127.8	130.3

$^{206}Pb/^{238}U$ weighted mean: 125.9 ± 1.2 Ma, MSWD = 1.2.

Table 3
$^{40}Ar/^{39}Ar$ data for groundmass of sample GW04137 from the Manitu Formation, by incremental technique.

Steps	T/°C	^{39}Ar accu./%	^{40}Ar/%	$^{36}Ar/^{39}Ar$	$^{37}Ar/^{39}Ar$	$^{40}Ar/^{39}Ar$	$^{40}Ar^*/^{39}Ar$	Age/Ma	2σ
01	780	8.96	24.31	0.1264	0.0112	48.79	11.87	114.44	14.60
02	840	16.51	26.39	0.1200	0.0104	47.64	12.58	121.03	13.48
03	890	21.16	41.04	0.0703	0.0152	34.17	14.02	134.41	8.35
04	940	24.99	60.40	0.0338	0.0283	22.27	13.46	129.21	5.47
05	990	27.57	76.95	0.0183	0.0226	18.91	14.44	138.21	4.14
06	1040	32.88	77.34	0.0159	0.0082	18.95	14.57	139.40	3.15
07	1080	37.28	76.26	0.0168	0.0075	19.27	14.58	139.51	3.10
08	1120	46.53	78.90	0.0127	0.0033	16.89	13.25	127.22	2.09
09	1150	54.21	78.65	0.0129	0.0032	16.92	13.21	126.92	2.57
10	1190	64.29	82.24	0.0103	0.0037	16.02	13.10	125.88	1.92
11	1240	77.01	82.39	0.0112	0.0088	16.72	13.75	131.86	1.91
12	1280	97.18	75.61	0.0201	0.0202	21.08	16.01	152.66	2.73
13	1330	98.78	61.31	0.0509	0.0506	33.32	20.56	193.82	6.48
14	1450	100.00	57.58	0.0562	0.0465	34.35	19.82	187.15	7.49

GW04137: Plateau age: 128.1 ± 3.1 Ma (MSWD = 7.4) Inverse isochron age: 128.6 ± 3.1 Ma (n = 4; MSWD = 11.3).
J value: 0.005502 ± 0.000028. Age of Bern4M is 18.7 ± 0.06 Ma.

degassing, were commonly 2–3 orders of magnitude smaller than sample signals. The mean blank errors were generally ~2% for ^{40}Ar and ~5% for ^{39}Ar. However, the large size of the samples relative to the blank minimized the impact of these errors propagating into the final ages. The plateau age was calculated from 3 or more contiguous steps, comprising >50% of the ^{39}Ar released, and gave concordant ages at the 95% confidence level. Errors are reported at the 2σ confidence level (Table 3).

5. Results

5.1. Manketouebo Formation

The Manketouebo Formation is traditionally considered as the lowest unit of the volcanic sequence in the southern Great Xing'an Range, which makes it essential to date this in order to constrain the onset of volcanism. Zircon from a total of 17 samples, including 9 rhyolites, 3 dacites, 2 andesites and 3 tuffaceous rocks, were dated by LA-ICPMS. For convenience, the age results of these samples are described according to their lithology.

Zircons from the nine rhyolites are discussed first and the data are plotted on concordia diagrams in Fig. 5. Sample 05FW060 from the southern part of the Wudan Basin is a porphyritic rhyolite with phenocrysts of sanidine dispersed in a fine-grained matrix. In the field, it has well-developed columnar joints. The data are concordant to slightly discordant and the weighted mean $^{206}Pb/^{238}U$ age of seven analyses is 174 ± 4 Ma (MSWD = 8.4; Fig. 5a), which is considered to be the eruption age of the rock; an older of age of 309 ± 3 Ma was obtained from a xenocryst. Samples 06ZH032 and 06ZH110 are both porphyritic rhyolites with phenocrysts of altered K-feldspar set in a felsitic matrix. Sample 06ZH032 from south of the Baoshi Basin is grey–purple in color and characterized by well-developed flow structure; with clusters of small quartz phenocrysts observed locally. The data are concordant and the weighted mean $^{206}Pb/^{238}U$ age of nineteen analyses is 133 ± 2 Ma (MSWD = 9.6; Fig. 5b). In addition to altered K-feldspar, sample 06ZH110 from the Wudan Basin also contains phenocrysts of embayed quartz and opaque minerals set in a fine-grained matrix. The data are mostly concordant and the weighted mean age of thirteen analyses is 154 ± 1 Ma (MSWD = 0.2; Fig. 5c). Sample 07ZH097 was collected from the western segment of the south Great Xing'an Range nearc Huolinhe. It is a grey, massive rhyolite with phenocrysts of K-feldspar. The data are concordant and the weighted mean age of eighteen analyses is 150 ± 2 Ma (MSWD = 2.1; Fig. 5d), which represents the crystallization age of the rock.

Samples 07ZH110 and II06029-1 were collected from the type section of the Manketouebo Formation in the southern part of the Baoshi Basin. Sample 07ZH110 is a felsitic rhyolite with well-developed flow structure, containing rare phenocrysts of altered alkali-feldspar and embayed quartz. Nineteen analyses of mostly concordant zircon yield a weighted mean age of 154 ± 1 Ma (MSWD = 0.3; Fig. 5e). Sample II06029-1 has oriented phenocrysts of broken alkali-feldspar and quartz set in a felsic matrix. Six analyses are slightly spread along concordia and give a weighted average $^{206}Pb/^{238}U$ age of 153 ± 8 Ma (MSWD = 4.0; Fig. 5f). One grain records an older age of 185 ± 4 Ma and is interpreted to be a xenocryst. Within errors, the ages of the two samples are identical, indicating their formation in the Late Jurassic.

Sample 07ZH172 was collected from the top of the Manketouebo Formation, immediately beneath the Manitu Formation at the type location of the latter, NE of Linxi. It is a massive rhyolite with a felsitic texture and is devoid of phenocrysts. Nineteen analyses yield a weighted mean age of 163 ± 1 Ma (MSWD = 0.1; Fig. 5g). Samples II06031-2 and II06032-1 are both porphyritic rhyolites, collected a few kilometers east of the previous site. Nineteen analyses of the former yield a weighted mean $^{206}Pb/^{238}U$ age of 160 ± 2 Ma (MSWD = 5.7; Fig. 5h). The weighted mean age of sixteen analyses of the latter is 165 ± 1 Ma (MSWD = 0.8; Fig. 5i) and both ages are taken to represent the eruption time of these rocks, indicating that the volcanic rocks of the Manketouebo Formation were erupted in the Late Jurassic.

Three samples of dacite (07ZH017, 07ZH155 and GW04199) were analyzed. Sample 07ZH017 from the northern part of the Baoshi Basin is a fine-grained, massive dacite with a few phenocrysts of plagioclase. The zircons are concordant and seventeen analyses yield a weighted mean age of 138 ± 1 Ma (MSWD = 0.2; Fig. 5j). Sample 07ZH155 from the northern part of the Pingshan Basin is a massive dacite, containing a large number of crystal fragments and a few fragments of chilled lava. The crystal fragments mainly comprise plagioclase, with minor quartz. The weighted mean age of ten concordant grains is 151 ± 1 Ma (MSWD = 1.2), considered to represent the time of eruption. One inherited grain yields an age of 177 ± 4 Ma (Fig. 5k). Sample GW04199 was collected north of the Baoshi Basin, close to the Mongolian border, and is a porphyritic dacite with phenocrysts of altered plagioclase, embayed quartz and rare biotite, set in a microcrystalline matrix. The data are mostly concordant and fourteen analyses yield a weighted mean $^{206}Pb/^{238}U$ age of 124 ± 2 Ma (MSWD = 2.7; Fig. 5l). Three other concordant grains define an older age of 168 ± 1 Ma (MSWD = 0.9), representing the age of a single population of inherited zircons.

Andesite sample 07ZH104 was collected from the western segment of the south Great Xing'an Range, immediately west of Huolinhe. The data are concordant and the weighted mean age of sixteen analyses is 157 ± 2 Ma (MSWD = 0.3; Fig. 5m). Sample

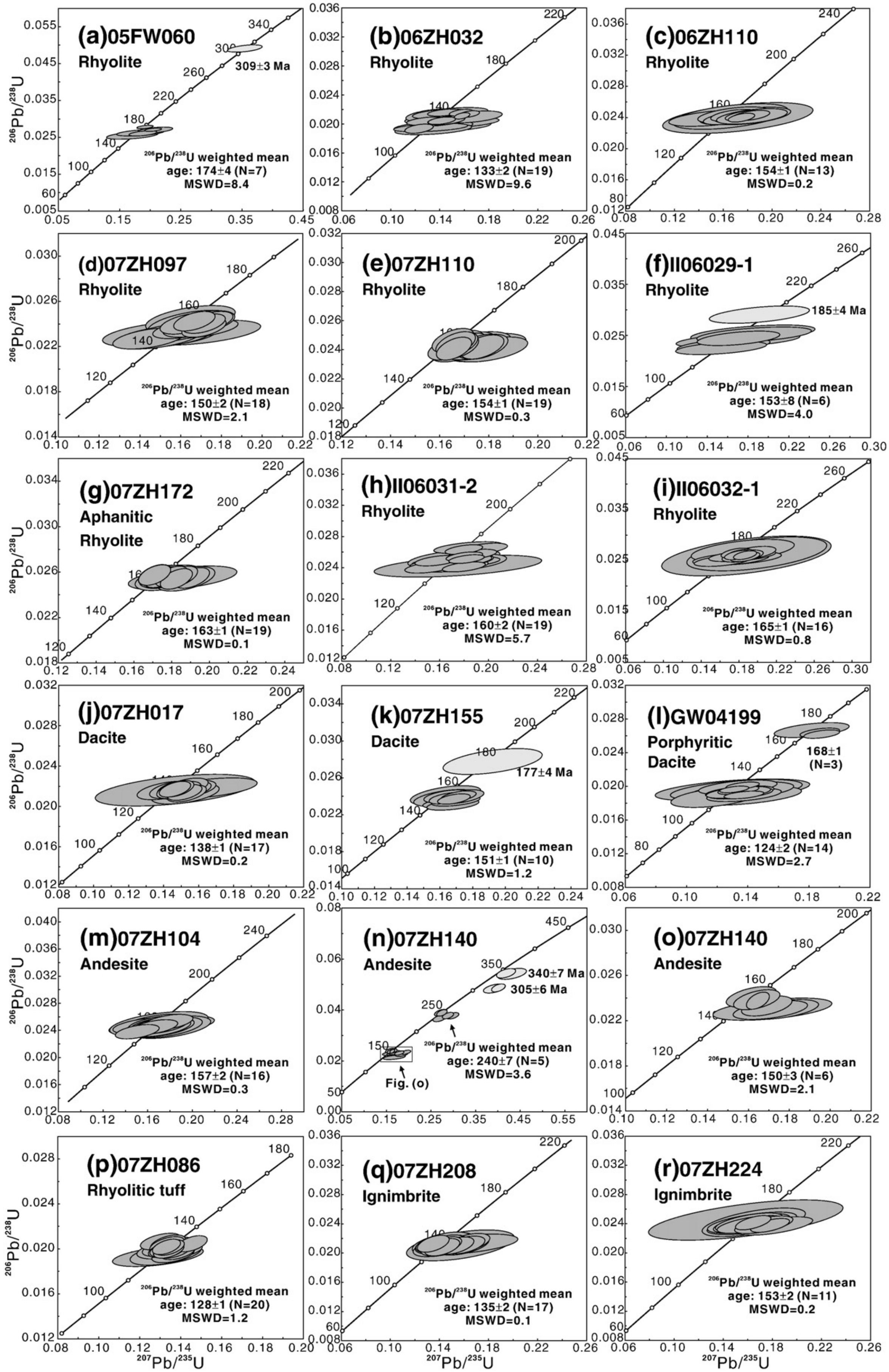
(a)05FW060
Rhyolite
309±3 Ma
²⁰⁶Pb/²³⁸U weighted mean age: 174±4 (N=7) MSWD=8.4
(b)06ZH032
Rhyolite
²⁰⁶Pb/²³⁸U weighted mean age: 133±2 (N=19) MSWD=9.6
(c)06ZH110
Rhyolite
²⁰⁶Pb/²³⁸U weighted mean age: 154±1 (N=13) MSWD=0.2
(d)07ZH097
Rhyolite
²⁰⁶Pb/²³⁸U weighted mean age: 150±2 (N=18) MSWD=2.1
(e)07ZH110
Rhyolite
²⁰⁶Pb/²³⁸U weighted mean age: 154±1 (N=19) MSWD=0.3
(f)II06029-1
Rhyolite
185±4 Ma
²⁰⁶Pb/²³⁸U weighted mean age: 153±8 (N=6) MSWD=4.0
(g)07ZH172
Aphanitic Rhyolite
²⁰⁶Pb/²³⁸U weighted mean age: 163±1 (N=19) MSWD=0.1
(h)II06031-2
Rhyolite
²⁰⁶Pb/²³⁸U weighted mean age: 160±2 (N=19) MSWD=5.7
(i)II06032-1
Rhyolite
²⁰⁶Pb/²³⁸U weighted mean age: 165±1 (N=16) MSWD=0.8
(j)07ZH017
Dacite
²⁰⁶Pb/²³⁸U weighted mean age: 138±1 (N=17) MSWD=0.2
(k)07ZH155
Dacite
177±4 Ma
²⁰⁶Pb/²³⁸U weighted mean age: 151±1 (N=10) MSWD=1.2
(l)GW04199
Porphyritic Dacite
168±1 (N=3)
²⁰⁶Pb/²³⁸U weighted mean age: 124±2 (N=14) MSWD=2.7
(m)07ZH104
Andesite
²⁰⁶Pb/²³⁸U weighted mean age: 157±2 (N=16) MSWD=0.3
(n)07ZH140
Andesite
340±7 Ma
305±6 Ma
²⁰⁶Pb/²³⁸U weighted mean age: 240±7 (N=5) MSWD=3.6
Fig. (o)
(o)07ZH140
Andesite
²⁰⁶Pb/²³⁸U weighted mean age: 150±3 (N=6) MSWD=2.1
(p)07ZH086
Rhyolitic tuff
²⁰⁶Pb/²³⁸U weighted mean age: 128±1 (N=20) MSWD=1.2
(q)07ZH208
Ignimbrite
²⁰⁶Pb/²³⁸U weighted mean age: 135±2 (N=17) MSWD=0.1
(r)07ZH224
Ignimbrite
²⁰⁶Pb/²³⁸U weighted mean age: 153±2 (N=11) MSWD=0.2
²⁰⁶Pb/²³⁸U
²⁰⁷Pb/²³⁵U

07ZH140 is an andesite from the Pingshan Basin and is much more complex, containing four zircon populations with ages of 150 ± 3 Ma, 240 ± 7 Ma, 305 ± 6 Ma and 340 ± 7 Ma (Fig. 5n and o), of which the 150 ± 3 Ma age is taken to represent the eruption age of the rock; the older grains being considered inherited.

Three tuffaceous rocks from the Manketouebo Formation were also dated. Twenty zircon analyses from sample 07ZH086, a rhyolitic tuff from the Tuliemaodu section in the east-central part of the Baoshi Basin, are mostly concordant and record a weighted mean $^{206}Pb/^{238}U$ age of 128 ± 1 Ma (MSWD = 1.2; Fig. 5p). This age can be taken as the time of eruption. Sample 07ZH208, a massive porphyritic ignimbrite from southeast of Keshiketengqi, contains K-feldspar megacrysts in a fine-grained matrix. The data for seventeen grains are concordant to weakly discordant and define a weighted mean age of 135 ± 2 Ma (MSWD = 0.1; Fig. 5q). Sample 07ZH224 from the nearby Wudan Basin is an ignimbrite with well-developed flow structure, containing some fragments of feldspar and quartz. The data are mostly concordant and eleven analyses define a weighted mean $^{206}Pb/^{238}U$ age of 153 ± 2 Ma (MSWD = 0.2; Fig. 5r), taken as the time of the eruption.

5.2. Manitu Formation

Stratigraphically, the Manitu Formation is a vital component of the volcanic sequence in the southern part of the Great Xing'an Range, since it has been used in discriminating the felsic volcanic rocks of the Manketouebo and Baiyingaolao formations, as discussed above. Nine samples of this formation, including andesites (5 samples), dacite (1 sample), rhyolite (1 sample) and a felsic tuffaceous rock (1 sample), were dated using LA-ICPMS (8 samples) and an additional sample of andesite was dated using the $^{40}Ar/^{39}Ar$ incremental heating technique.

Sample 07ZH006 from the northern part of the Baoshi Basin is a porphyritic andesite with phenocrysts of plagioclase and rare hornblende, set in an aphanitic matrix. Nineteen concordant to slightly discordant analyses yield a weighted mean $^{206}Pb/^{238}U$ age of 151 ± 2 Ma (MSWD = 1.7; Fig. 6a). There are also two concordant inherited grains with ages of 212 ± 3 Ma and 230 ± 4 Ma. Sample 07ZH181 is a fine-grained andesite collected from the upper section of the Manitu Formation at the type location, NE of Linxi. It is characterized by a well-developed flow structure. Analyses of eighteen concordant zircons yield a weighted mean age of 138 ± 1 Ma (MSWD = 0.1; Fig. 6b). One inherited zircon has a $^{206}Pb/^{238}U$ age of 306 ± 5 Ma.

Sample 06ZH049 from southwest of the Pingshan Basin is a porphyritic pyroxene andesite with phenocrysts of plagioclase and orthopyroxene. Most of the plagioclase and some of the pyroxene is altered. Twenty concordant analyses record a weighted mean age of 132 ± 1 Ma (MSWD = 0.6; Fig. 6c). Sample G0221-2 was collected from the eastern margin of the Great Xing'an Range, southwest of the Pingshan Basin. It is a hornblende andesite with plagioclase and amphibole phenocrysts dispersed in a fine-grained matrix. Eleven concordant grains yield an age of 129 ± 2 Ma (MSWD = 1.2). In addition, four analyses form a coherent population that yields a weighted mean age of 197 ± 4 Ma (MSWD = 0.3) (Fig. 6d). The younger population is considered to record the age of the volcanic eruption, whereas the older population represents inheritance from a single source. Sample GW04136 is also from the eastern margin of the Great Xing'an Range, to the east of the Baoshi Basin. It is a massive porphyritic pyroxene andesite that contains a few phenocrysts of pyroxene and plagioclase, with rare biotite and hornblende. The weighted mean age of thirteen grains is 125 ± 1 Ma (MSWD = 3.3) (Fig. 6e), which is taken to record the age of the andesite.

Sample 07ZH236 is a porphyritic dacite from the Wudan Basin that contains phenocrysts of plagioclase and rare hornblende. The data are mostly concordant and the weighted mean age of thirteen analyses is 156 ± 1 Ma (MSWD = 1.1) with one inherited grain yielding an older age of 272 ± 3 Ma (Fig. 6f). Sample 07ZH193 is a massive white porphyritic rhyolite from east–northeast of Linxi. The main phenocryst phase is euhedral quartz dispersed in a fine-grained groundmass. The data are concordant to slightly discordant and eleven analyses yield a weighted mean age of 155 ± 1 Ma (MSWD = 0.1; Fig. 6g). Sample 07ZH081 from the eastern margin of the Baoshi Basin is a rhyolitic tuff, with crystal fragments of feldspar and quartz. The data are concordant and nineteen analyses yield a weighted mean age of 126 ± 1 Ma (MSWD = 1.2; Fig. 6h).

The fine-grained groundmass of pyroxene andesite sample GW04137, collected near the eastern margin of the Great Xing'an Range, southwest of Wulan Hot, was dated by the $^{40}Ar/^{39}Ar$ incremental heating method. In the initial heating steps, the plateau ages increase with increasing temperature, which may be caused by release of absorbed Ar from the surface or subsurface of the sample. However, the plateau became homogeneous at the temperature interval between 1120 C and 1240 C. The calculated plateau age of these four steps (128.1 ± 3.1 Ma, including about 40% released ^{39}Ar), and the calculated inverse isochron age (128.6 ± 3.1 Ma) are identical (Fig. 6i, j). The deduced $^{40}Ar/^{36}Ar$ ratio is 291.8, indicating no adsorbed excess Ar in the sample. Therefore, this age is taken to represent the time of crystallization.

5.3. Baiyingaolao Formation

The Baiyingaolao Formation comprises a suite of felsic volcanic and related volcanoclastic rocks of great thickness. Nine samples, including rhyolites (6 samples), dacite (1 sample) and felsic ignimbrites (3 samples), were dated by LA-ICPMS and one sample by TIMS.

Three transparent prismatic zircons from rhyolite sample 436, obtained from the northern end of the study area near Arshan, were dated by TIMS. They are concordant and yield an age of 125.9 ± 1.2 Ma (MSWD = 1.2; Fig. 7a), which represents the age of the rock.

Samples 06ZH015, 06ZH043 and 06ZH055 are rhyolite dated by LA-ICPMS. Sixteen concordant to weakly discordant analyses of sample 06ZH015 from northeast of Linxi give a weighted mean age of 131 ± 1 Ma (MSWD = 1.1; Fig. 7b); whereas the weighted mean age of twelve concordant to weakly discordant grains in sample 06ZH043 from the southern part of the Baoshi Basin is 129 ± 1 Ma (MSWD = 3.4; Fig. 7c). Twenty zircon analyses of massive felsite sample 06ZH055 from the Pingshan Basin are concordant and yield a weighted mean age of 132 ± 1 Ma (MSWD = 0.7; Fig. 7d).

Two additional rhyolite samples were collected from the northernmost part of the southern Great Xing'an Range (Fig. 1c). Sample GW04185 collected west of the Baoshi Basin is a porphyritic rhyolite with sanidine and quartz phenocrysts set in a felsitic groundmass, and characterized by well-developed flow structure and local clusters of recrystallized quartz. Concordant zircons form three age clusters with weighted mean ages of 135 ± 1 Ma (N = 15; MSWD = 1.9), 161 ± 4 Ma (N = 2) and 290 ± 25 Ma (N = 2), respectively (Fig. 7e). The youngest age of 135 ± 1 Ma is taken as the age of the rock, whereas the older grains are interpreted as being inherited. There are also some discordant younger ages, but their geological significance is uncertain. Sample GW04215 from Arshan is a massive porphyritic

Fig. 5. Zircon LA-ICPMS U–Pb concordia diagrams of volcanic rocks from the Manketouebo Formation. (a) 05FW060; (b) 06ZH032; (c) 06ZH110; (d) 07ZH097; (e) 07ZH110; (f) II06029-1; (g) 07ZH172; (h) II06031-2; (i) II06032-1; (j) 07ZH017; (k) 07ZH155; (l) GW04199; (m) 07ZH104; (n and o) 07ZH140; (p) 07ZH086; (q) 07ZH208; (r) 07ZH224.

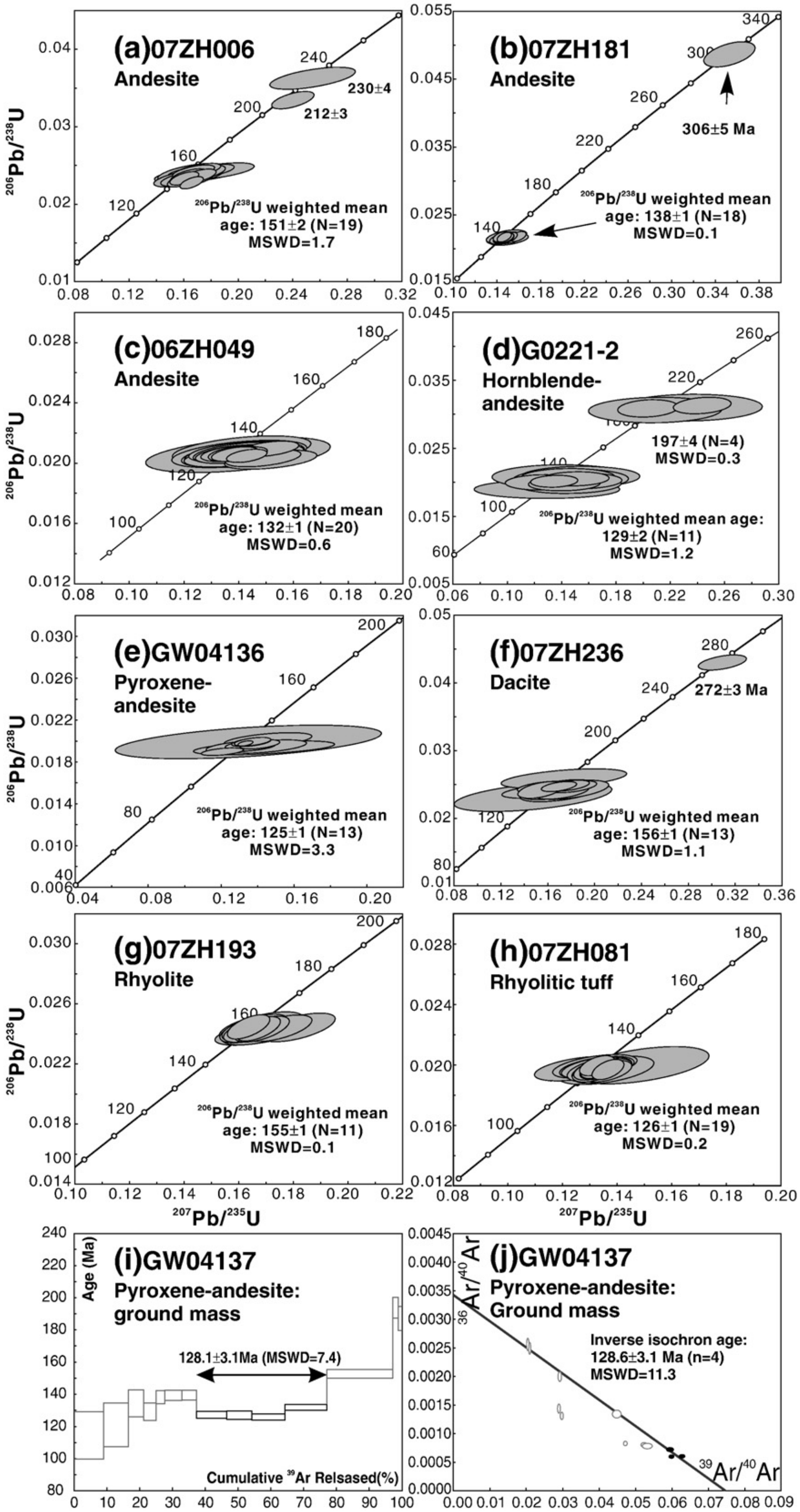

Fig. 6. Geochronological diagrams of volcanic rocks from the Manitu Formation. LA-ICPMS zircon U–Pb age concordia diagrams of (a) 07ZH006, (b) 07ZH181, (c) 06ZH049, (d) G0221-2, (e) GW04136, (f) 07ZH236, (g) 07ZH193, (h) 07ZH081; (i) $^{40}Ar/^{39}Ar$ age spectra and (j) inverse isochron of the groundmass of GW04137.

rhyolite with a few quartz phenocrysts set in a felsitic matrix. Twenty-four analyses are mostly concordant and yield a weighted mean age of 124 ± 1 Ma (MSWD = 1.1; Fig. 7f). This age is taken as the eruption age of the rock.

Sample 07ZH078 from the central part of the Baoshi Basin is a massive porphyritic dacite with plagioclase phenocrysts. Twenty analyses of concordant to slightly discordant zircon record a weighted mean $^{206}Pb/^{238}U$ age of 131 ± 1 Ma (MSWD = 1.4; Fig. 7g). Sample

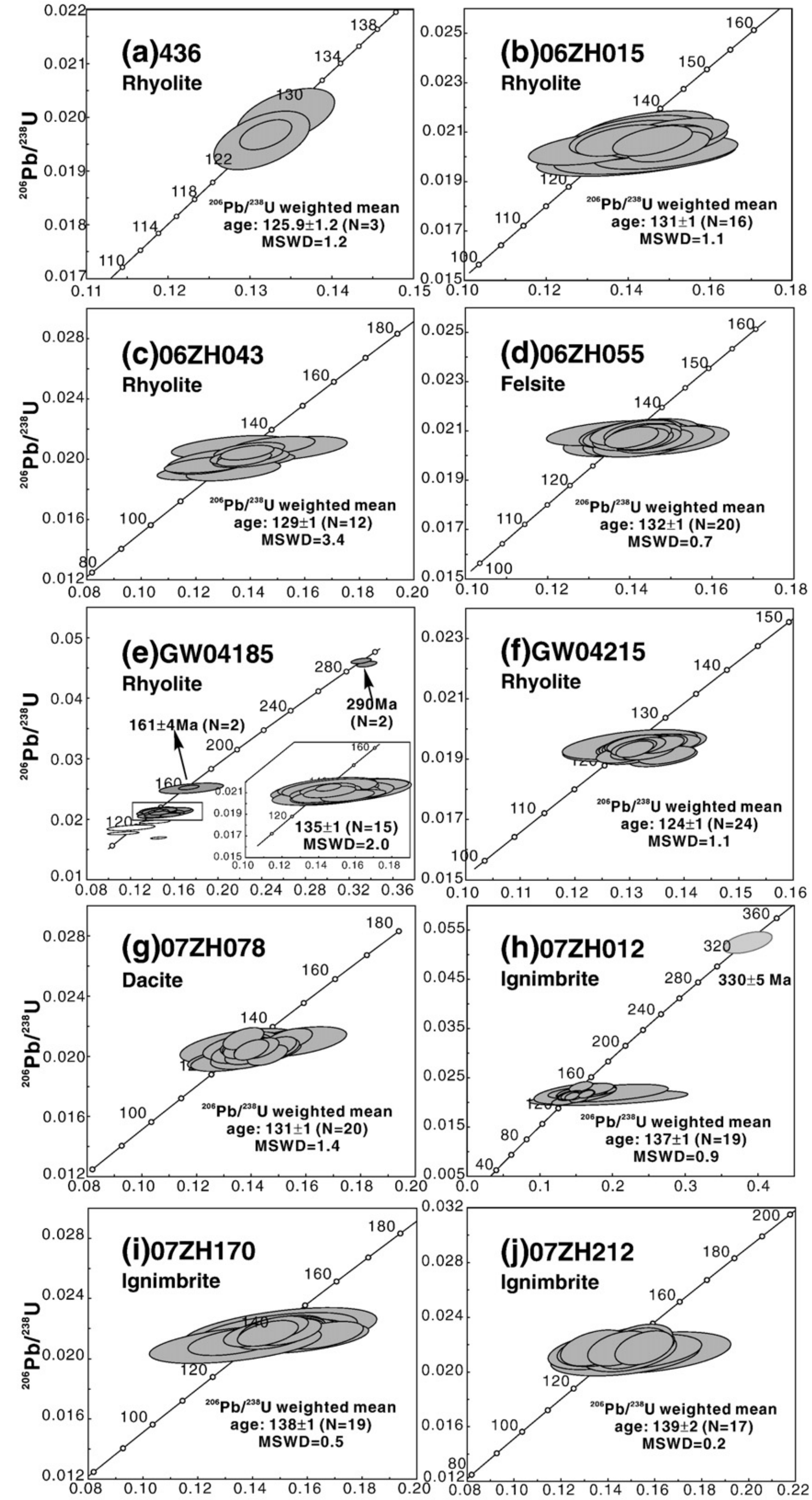

Fig. 7. Zircon U–Pb concordia diagrams of volcanic rocks from the Baiyingaolao Formation. (a) 436; (b) 06ZH015; (c) 06ZH043; (d) 06ZH055; (e) GW04185; (f) GW04215; (g) 07ZH078; (h) 07ZH012; (i) 07ZH170; (j) 07ZH212. TIMS age for sample 436; all other ages were determined by LA-ICPMS.

07ZH012 from the northern part of the Baoshi Basin is a purple–red ignimbrite with abundant K-feldspar and quartz fragments of various sizes. Nineteen concordant or near concordant analyses give a weighted mean age of 137 ± 1 Ma (MSWD = 0.9; Fig. 7h). One grain also has an older age of 330 ± 5 Ma and is inherited. Sample 07ZH170 is a welded ignimbrite with crystal fragments of plagioclase and quartz, collected from the type location of the Baiyingaolao Formation, northeast of Linxi. The weighted mean age of nineteen concordant analyses is 138 ± 1 Ma (MSWD = 0.5; Fig. 7i). Sample 07ZH212 from near Keshiketengqi is an aphanitic felsitic ignimbrite. Seventeen concordant to weakly

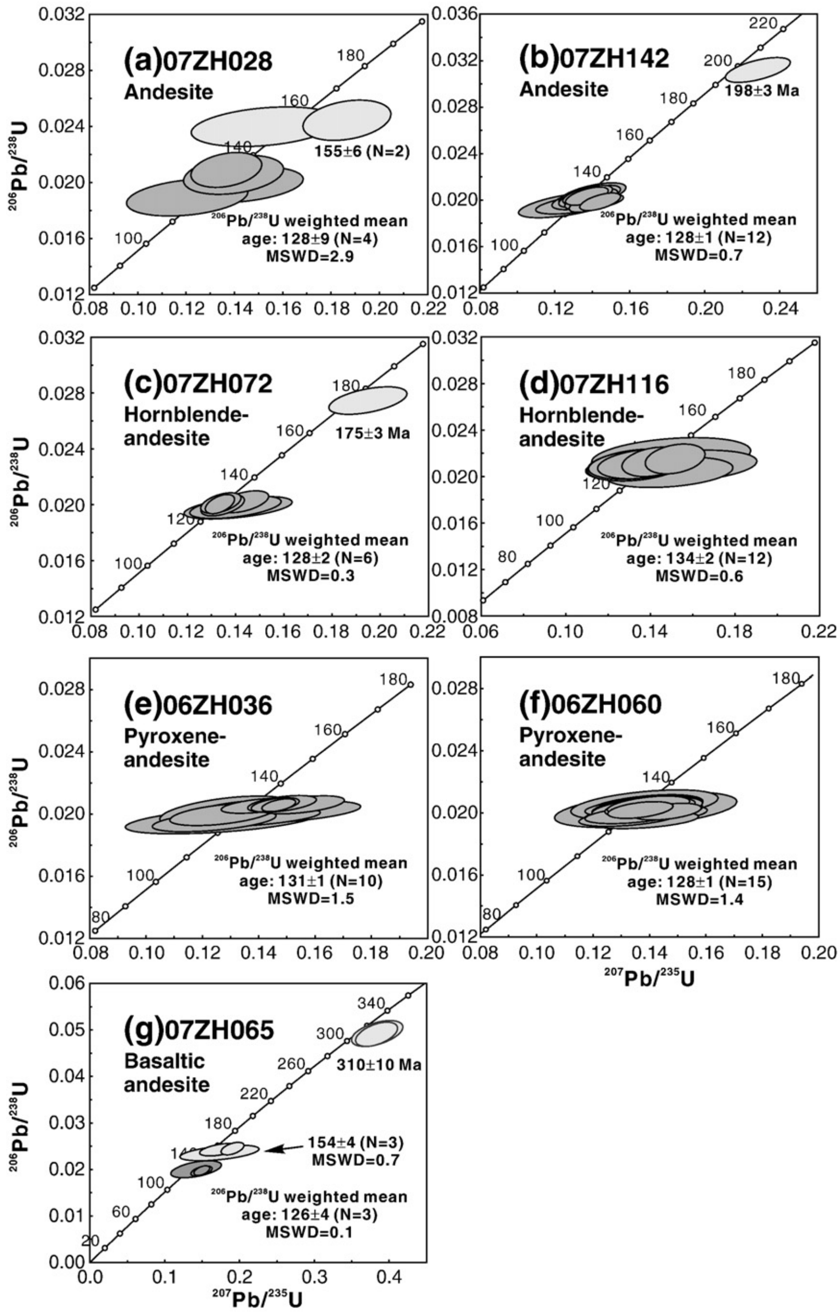

Fig. 8. Zircon LA-ICPMS U–Pb age concordia diagrams for andesites from the Meiletu Formation. (a) 07ZH0280; (b) 07ZH142; (c) 07ZH072; (d) 07ZH116; (e) 6ZH036; (f) 06ZH060; (g) 07ZH065.

discordant analyses yield a weighted mean age of 139 ± 2 Ma (MSWD = 0.2; Fig. 7j), interpreted as the age of eruption.

5.4. Meiletu Formation

The Meiletu Formation is the uppermost unit of the volcanic sequence recognized in the south Great Xing'an Range and its age will constrain the termination of volcanism in the region. A total of seven andesites were dated by LA-ICPMS.

Sample 07ZH028 from the northern part of the Baoshi Basin is a fine-grained andesite with a few hornblende phenocrysts. Four concordant zircons from this sample yield a weighted mean age of 128 ± 9 Ma (MSWD = 2.9) which is considered the age of volcanic eruption. Two zircons record older ages of 155 ± 6 Ma (Fig. 8a), taken to record inheritance. Sample 07ZH142 from the Pingshan Basin is a massive porphyritic andesite with plagioclase phenocrysts. Twelve concordant analyses yield a weighted mean age of 128 ± 1 Ma (MSWD = 0.7; Fig. 8b). One inherited grain gives a $^{206}Pb/^{238}U$ age of 198 ± 3 Ma. Zircons from sample 07ZH072 from the Baoshi Basin near Baoshi are mostly concordant and six analyses record a weighted mean age of 128 ± 2 Ma (MSWD = 0.3; Fig. 8c), with one inherited zircon recording an age of 175 ± 3 Ma. Twelve concordant analyses of hornblende-andesite sample 07ZH116, collected between the Baoshi and Pingshan basins, record a weighted mean age of 134 ± 2 Ma (MSWD = 0.6; Fig. 8d).

Sample 06ZH036 was collected from the type location of the Meiletu Formation in the southern part of the Baoshi Basin and is a massive pyroxene andesite, with well-developed columnar jointing. Ten analyses are concordant to weakly discordant and record a weighted mean age of 131 ± 1 Ma (MSWD = 1.5; Fig. 8e). Sample 06ZH060 was collected between the Baoshi and Pingshan basins, in close proximity to

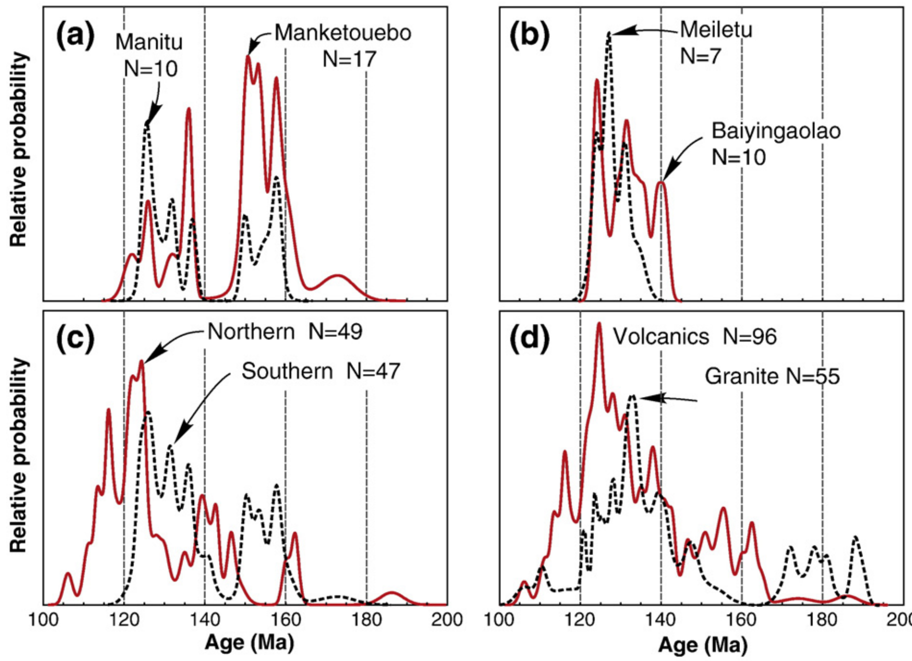

Fig. 9. Probability diagrams of the volcanic rocks and granites in the Great Xing'an Range: (a) The Manketouebo and Manitu formations; (b) the Baiyingaolao and Meiletu formations; (c) comparison of the age frameworks of the volcanic rocks in the northern and southern segments of the Great Xing'an Range; and (d) comparison of the ages of the volcanic rocks and granites in the Great Xing'an Range.

sample 07ZH116. It is a biotite-bearing pyroxene andesite and fifteen concordant zircon analyses record a weighted mean age of 128 ± 1 Ma (MSWD = 1.4; Fig. 8f). Sample 07ZH065 is an aphanitic basaltic andesite collected near the eastern margin of the Great Xing'an Range, southeast of Baoshi. Three analyses record a weighted mean age of 126 ± 4 Ma, and this is taken to record the time of volcanism, since they form rims to older grains. In addition, three zircons define a weighted mean age of 154 ± 4 Ma (Fig. 8g) and two zircons record an even older age of 310 ± 10 Ma and are considered to be inhered.

6. Discussion

6.1. Geochronological framework of the volcanic rocks and constraints on the volcanic stratigraphy

The large range in crystallization age of all four volcanic formations indicates that the subdivision and correlation of these volcanic strata needs to be re-evaluated. For instance, samples from the Manketouebo Formation, which is considered to be the lowermost unit, show a total age range from 174 ± 4 Ma to 124 ± 2 Ma, the overlying Manitu Formation a range from 156 ± 1 Ma to 125 ± 1 Ma, the succeeding Baiyingaolao Formation from 139 ± 2 Ma to 124 ± 1 Ma and the believed uppermost Meiletu Formation a range from 134 ± 2 Ma to 126 ± 4 Ma. This is clearly impossible in a true stratigraphic sequence and indicates that previous correlations across the area are incorrect. Only the upper Meiletu Formation shows a consistent range of younger ages. However, all other formations contain rocks with zircon ages within this same time-frame, emphasizing the problems of the previous subdivision, which was mainly based on correlation of rock assemblages, with few isotopic age data. Our new data indicate that this approach cannot be supported. In addition, felsic rocks of the Manketouebo and Baiyingaolao Formations are indistinguishable in terms of lithology and geochemistry (refer to Fig. 4b) and the new age data indicate that some sequences previously mapped as Manketouebo Formation could equally belong to the Baiyingaolao Formation. This unsatisfactory situation with respect to the stratigraphic subdivision is also manifested by the age results from a single volcanic basin. For example, in the Hatumohe section in the Baoshi Basin, the so-called Manitu Formation is older than what was classified as lowermost Manketouebo Formation, while in the Tuliemaodu, Paotai and Keshiketengqi sections, volcanic rocks considered to be in different formations have the same ages within errors.

Another important point is the regional correlation of volcanic strata across the whole of the Great Xing'an Range. Previous studies considered that the volcanic rocks in the northern segment were older than those in the southern region (HBGMR, 1993; IMBGMR, 1991; Wang et al., 1997; Fig. 3) due to the absence of a lower mafic volcanic unit that could be correlated with the Tamulangou Formation in the northern segment. However, our data indicate that initiation of volcanism in the Late Jurassic was synchronous across the whole of the Great Xing'an Range (see also Zhang et al., 2008b).

The volcanic rocks in the Great Xing'an Range were previously considered to be Late Jurassic to Early Cretaceous based on imprecise age data. Recent studies show that the majority of the dated volcanic rocks in the northern segment erupted in the Early Cretaceous, with a minority erupted in the Late Jurassic; and mostly in the west of the northern Great Xing'an Range (Ge et al., 2001; Wu et al., 2005d; Chen et al., 2006; Wang et al., 2006b; Zhang et al., 2008b). Nevertheless, precise age data for the volcanic rocks in the southern segment were previously limited (Chen et al., 2007; Guo et al., 2008). Our new age data for 43 volcanic rocks from the four major Mesozoic volcanic units across the entire southern Great Xing'an Range confirms that volcanic rocks erupted in both the Late Jurassic and Early Cretaceous. Compilation of the available ages shows two stages of volcanism in the southern Great Xing'an Range, i.e., in the Late Jurassic at 160–150 Ma and in the Early Cretaceous at 141–122 Ma, with a distinct time-gap between them (Chen et al., 2007; Guo et al., 2008). Thus, both the northern and southern segments have Late Jurassic and the Early Cretaceous volcanic rocks, with the climax in the Early Cretaceous, consistent with the giant igneous event recognized in other parts of eastern China by Wu et al. (2005a). However, the age data indicate that Jurassic volcanic rocks form a relatively subordinate proportion of the rocks, although erosion prior to eruption of the Early Cretaceous rocks may have contributed to this. The Great Xing'an Range therefore is an important component of the giant Cretaceous igneous event. But although the Early Cretaceous rocks are dominant, Late Jurassic rocks occupy a relative larger proportion in the southern segment compared to the north (Fig. 9c). Volcanism in the northern segment includes four stages, i.e., at ~180 Ma, 165–160 Ma, 150–135 Ma and 130–105 Ma with a gap between 160 Ma and 150 Ma (Zhang et al., 2008b and references therein; Fig. 9c). In contrast, the southern segment contains just three stages, i.e., at ~173 Ma, 160–150 Ma and 141–122 Ma, with a gap between 150 ma and 141 ma. It is also evident that volcanism in the southern segment occurred when there was quiescence in northern segment (Fig. 9c). The other difference is the duration of the volcanism. In the southern segment, volcanism ended at about 122 Ma, whereas in the southern segment, it lasted to 105 Ma. This disparity between the northern and southern segments was probably caused by fundamental tectonic differences, which are discussed in the following section.

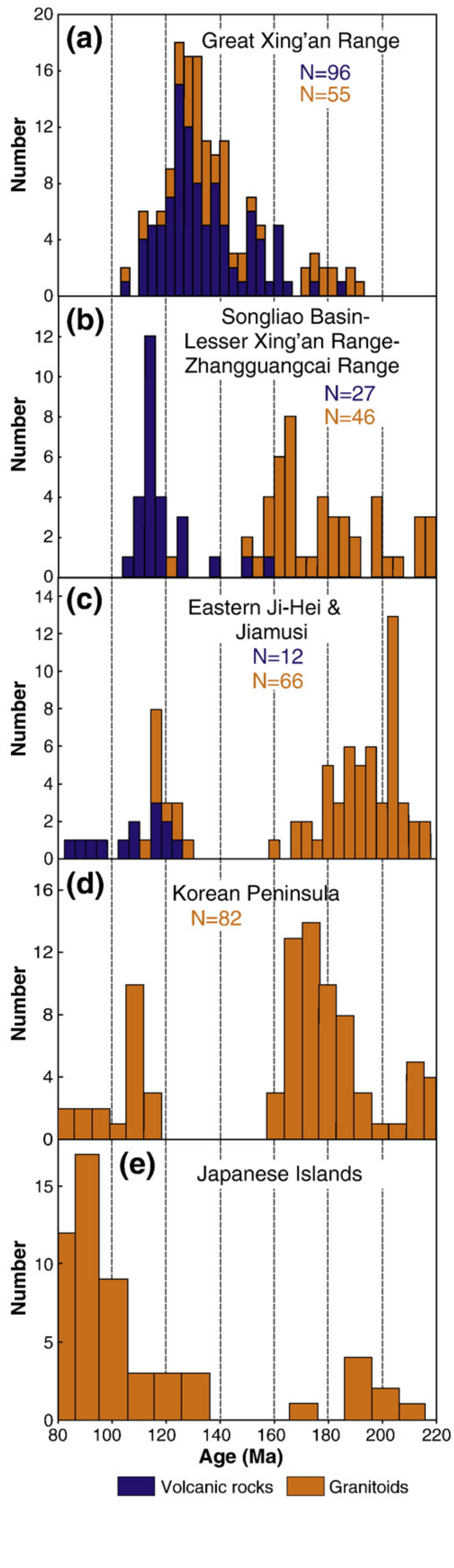

6.2. Temporal and spatial variations of Mesozoic magmatism in the Great Xing'an Range and adjacent regions

Besides the Great Xing'an Range, Mesozoic volcanic rocks are also widespread in other parts of northeastern China, including the Songliao Basin, the Zhangguangcai Range, and the eastern part of the Jilin and Heilongjiang Provinces (eastern Ji-Hei for short), as well as the Jiamusi Massif (refer to Fig. 1). In the Songliao Basin, the Mesozoic volcanic rocks are commonly intercalated with sedimentary sequences, as revealed by boreholes and outcrops. They have Early Cretaceous ages of 140–106 Ma (Wang et al., 2002; Zhang et al., 2007b; Shu et al., 2007; Ding et al., 2007; Gao, 2008). The $^{40}Ar/^{39}Ar$ ages of volcanic rocks from the Zhangguangcai Range range from 126 to 117 Ma, i.e., Early Cretaceous (Li, 2006a; Fig. 10b). In eastern Ji-Hei and the Jiamusi Massif, Early Cretaceous volcanism has Ar–Ar and zircon U–Pb ages between 122.7 and 88.2 Ma (Ji et al., 2005; Ji, 2007; Li et al., 2007; Fig. 10c). Overall, Early Cretaceous volcanic rocks are dominant over Jurassic rocks in northeastern China. Compilation of these data shows an eastward temporal migration of volcanism across NE China (Wang et al., 2006b). Likewise, Mesozoic volcanism displays a trend of decreasing age from the Great Xing'an Range in the west to the Eastern Ji-Hei belt and Jiamusi Massif in the east.

Mesozoic granitoids are also widespread in northeastern China and cover at least 50% of the area in the mountainous regions. Most of them are I-type or peralkaline A-type (Wu et al., 2000a, 2002, 2003b; Ge et al., 2005b, 2007a; Sui et al., 2007). In the west, the granites in the Great Xing'an Range and the Manzhouli (refer to Fig. 1a) area are mainly Early Cretaceous in age, with minor Jurassic plutons (Wang and Zhao, 1997; Qin et al., 1999; Jahn et al., 2001; Wu et al., 2002, 2003b; Lin et al., 2004; Liu et al., 2005b; Ge et al., 2005b, 2007b; Sui et al., 2007; unpublished data of Wu FY; Fig. 10a). Jurassic granites are also reported in the basement of the Songliao sedimentary basin and adjacent regions (Wu et al., 2000b, 2001; Gao et al., 2007; Xu et al., 2008c). To the east of the Songliao Basin, the granites in the Zhangguangcai and Lesser Xing'an Range are Jurassic in age (Wu et al., 1998, 2000a; Sun, 2001; Sun et al., 2001a,b; Wu et al., 2002, 2004b;Miao et al., 2004; Sun et al., 2005a,b; Ge et al., 2007b; Fig. 10b). The granites in the eastern Ji-Hei belt and Jiamusi Massif were also mainly emplaced in the Jurassic with rare Early Cretaceous and Late Triassic rocks (Zhang et al., 2002b,2004; Wu et al., 2004a; Cheng et al., 2006; Zhang et al., 2007c; Fig. 10c). These age data indicate that Jurassic granitoids define a westward younging trend from the Eastern Ji-Hei Belt and Jiamusi Massif to the Great Xing'an Range, opposite to that of the volcanic rocks (Fig. 10). Note that the limited data

Fig. 10. Compilation of age data of volcanic rocks and granites from the Great Xing'an Range and adjacent regions. (a) the Great Xing'an Range (volcanic rocks: Ge et al., 2001; Wu et al., 2005d; Chen et al., 2006; Wang et al., 2006b; Zhang et al., 2006a,b; Chen et al., 2007; Guo et al., 2008; Zhang et al., 2008b and the present study; granites: Wang and Zhao, 1997; Qin et al., 1999; Jahn et al., 2001; Wu et al., 2002, 2003b; Lin et al., 2004; Ge et al., 2005b; Liu et al., 2005b; Sui et al., 2007; Ge et al., 2007b; unpubl. data of Wu FY); (b) the Songliao Basin-Lesser Xing'an Range-Zhangguangcai Range (volcanic rocks: Wang et al., 2002; Li, 2006b; Zhang et al., 2007b; Shu et al., 2007; Ding et al., 2007; Gao, 2008; granites: Wu et al., 1998; Wu et al., 2000a,b; Sun, 2001; Sun et al., 2001a,b; Wu et al., 2001, 2002; Miao et al., 2004; Wu et al., 2004b; Sun et al., 2005a,b; Ge et al., 2007b; Gao et al., 2007; Xu et al., 2008c); (c) the eastern Jilin–Heilongjiang Provinces and Jiamusi Massif (volcanic rocks: Ji et al., 2005; Ji, 2007; Li et al., 2007; granites: Zhang et al., 2002b, 2004; Wu et al., 2004a; Cheng et al., 2006; Zhang et al., 2007c); (d) the Korean Peninsula (Sagong et al., 2005; Wu et al., 2007b; and references therein); (e) the Japanese islands (modified from Sagong et al., 2005).

from Japan (Fig. 10e) are more equivocal and indicate a mainly Cretaceous age for granite plutonism.

If the igneous rocks in the Korean Peninsula and Japan are taken into account, the above-mentioned trends become more significant, despite comparable age data on the volcanic rocks being largely absent (Kinoshita, 1995; Sagong et al., 2005; Wu et al., 2007b; and references therein; Fig. 10d, e). In the Korean Peninsula, Jurassic and older granites are widespread, with ages ranging between >220 Ma and 158 Ma; while emplacement of the Early Cretaceous granitoids defines a maximum at about 115 Ma (Sagong et al., 2005; Wu et al., 2007b and references therein; Fig. 10d). For the Japanese islands, the emplacement of Early Cretaceous granitoids started at about 140 Ma, with the peak age at ~90 Ma; whilst the age of the Jurassic granites are mostly older than 180 Ma (Sagong et al., 2005; Fig. 10e). Although the ages of associated volcanic rocks in Korea and Japan are not available, the data clearly indicate two stages of magmatism, as in China.

This age compilation indicates that the Mesozoic igneous event in northeastern China and adjacent regions consists of two important episodes, i.e., in the Jurassic and the Early Cretaceous (Fig. 10). In the Zhangguangcai and Lesser Xing'an Ranges and in eastern Ji-Hei, volcanism was predominantly in the Cretaceous and granite plutonism in the Jurassic (Fig. 10b). On the contrary, in the Great Xing'an Range, volcanic and granitic rocks formed in both periods (Figs. 9d and 10a), but were predominantly formed in the Cretaceous. It is also evident that the initiation of magmatism in the Early Cretaceous was similar at about 130 Ma or slightly younger in all places except the Great Xing'an Range. However, even here the initial time of magmatism is not older than 145 Ma (Fig. 9). In the Korean Peninsula and Japan, Mesozoic magmatism also comprises two episodes, which is reflected by the ages of granitoids; unfortunately, no comparable data for volcanic rocks are available. Taken together, these data thus indicate a westward younging trend of the Jurassic granitoids in northeastern China and adjacent regions from the Pacific plate margin to the continental interior (Fig. 10). A similar trend is also found in the eastern segment of the North China Craton and south China and adjacent regions along the East Asia continental margin (Kinoshita, 1995; Zhou and Li, 2000; Zhou, 2003; Chen et al., 2005; Sagong et al., 2005; Wu et al., 2005b, 2007b). However, the Early Cretaceous volcanic rocks in northeastern China and the granites in the Korean peninsula and Japan display an opposite trend, becoming younger from the continental interior to the continental margin. It is also clear from Fig. 10 that, except for the Great Xing'an Range, the gap between the episodes of Jurassic and Cretaceous magmatism becomes larger from the continental interior to the continental margin (Fig. 10): this trend is more obvious if the peak age of magmatism is taken. In the Great Xing'an Range, there is no obvious gap between the two episodes (less than 10 Ma because of the shift in the 'magma gap' between volcanism and plutonism in the northern and southern parts of the range), while the gap is ~10 Ma, ~20 Ma, ≥40 Ma for the Songliao Basin-Lesser Xing'an Range-Zhangguangcai Range (eastern part of the Songliao Block), Eastern Ji-Hei and Jiamusi, and Korean–Japan, respectively. Noticeably, quiescence in magmatism occurs at ~150 Ma in all these areas except the Great Xing'an Range, which is coincident with the time of a major tectonic change in eastern China (e.g., Zhai et al., 2004), i.e., from compression to extension.

6.3. Tectonic implications

The present data, when combined with previous studies, indicate the predominance of Early Cretaceous volcanism in the Great Xing'an Range, with a relatively small proportion of Late Jurassic volcanic rocks and an age gap of <10 Ma between these two episodes. An obvious question is whether all these volcanic rocks formed in a common tectonic setting. Several lines of evidence suggest that the Late Jurassic and Early Cretaceous volcanic rocks formed in different tectonic environments (e.g., Wu and Sun, 1999; Wu et al., 2000a, 2002, 2003a; Ge et al., 2005b), that is, compressive in the Jurassic and extensional in the Cretaceous. It is generally considered that all the Early Cretaceous igneous rocks in northeastern China and adjacent areas formed in an extensional environment (Ge et al., 2001; Guo et al., 2001; Shao et al., 2001a,b; Fan et al., 2003; Lin et al., 2003; Gao et al., 2005; Wu et al., 2005a; Zhang et al., 2008b,c). This is evidenced by the presence of Early Cretaceous A-type granite and alkali rhyolite (Li and Yu, 1993; Wang and Zhao, 1997; Ge et al., 2001; Jahn et al., 2001; Lin et al., 2003; Wu et al., 2002; Ge et al., 2005b), metamorphic core complexes (Yang et al., 1996; Zhang et al., 1998; Liu et al., 2005a; Yang et al., 2007a; Donskaya et al., 2008) and coeval bimodal mafic and felsic dykes (Shao et al., 1998, 2001a,b; Shao and Zhang, 2002; Zhang et al., 2006a,b), as well as the development of extensional basins, such as the Songliao Basin (Meng, 2003). In fact, most of eastern China, including northeastern China, the eastern North China and Yangtze cratons and southeastern China, were characterized by extension in the Early Cretaceous (e.g., Zhou and Li, 2000; Zhou et al., 2003; Zhai et al., 2004; Lin and Wang, 2006).

In contrast, it is widely considered that northeastern China (e.g., Meng, 2003; Wu et al., 2005b; Ge et al., 2005b; Sui et al., 2007; Yang et al., 2007b) including the Yanshanian fold and thrust belt (e.g., Davis et al., 2001), were dominated by regional compression in the Jurassic. Supporting evidence includes development of an active continental margin (Wu et al., 2005b; Ge et al., 2005b; Sui et al., 2007) and the occurrence of adakitic rock associations (Gao et al., 2004, 2005; Zhang et al., 2006c; Sui et al., 2007). Meng (2003) suggested that during the Late Jurassic, the NE CAOB and the northern NCC underwent significant N–S compression, resulting in crustal shortening and thickening, related to the amalgamation between the NCC and Siberian plate. However, the age framework and the distribution of igneous rocks and Jurassic accretionary complexes along the continental margin do not support this interpretation. For example, it is that unreasonable the NNE-trending igneous belt was the result of N–S amalgamation; instead it argues for its connection with subduction of the Paleo-Pacific plate beneath the eastern Asia continent. Additional evidence supporting an E–W compressional regime comes from the development of Jurassic adakitic rocks in the Great Xing'an Range, although the precise age of these is not well constrained (Gao et al., 2005; Zhang et al., 2006c).

These above lines of evidence indicate that the tectonic environment changed from compressional in the Late Jurassic to extensional in the Early Cretaceous: the magmatic quiescence coincides with this tectonic transformation. We therefore suggest that the change occurred first at the end of the Jurassic in the Great Xing'an Range and migrated eastward, reflected by the onset of Early Cretaceous magmatism.

6.4. A subduction-induced delamination model

Several mechanisms have been proposed to explain the genesis of Mesozoic volcanic rocks in the Great Xing'an Range and adjacent regions in NE China, including (1) mantle plume or some other intraplate processes (Shao et al., 1995, 1999, 2001a,b; Deng et al., 1996; Lin et al., 1998; Ge et al., 1999), (2) post-orogenic lithospheric extension related to the closure of the Mongol–Okhotsk Ocean (Fan et al., 2003; Meng, 2003), and (3) westward subduction of the Paleo-Pacific plate and subsequent related processes, such as rifting (Jiang and Quan, 1988), asthenospheric upwelling (Zhao et al., 1989), and delamination (Wang et al., 2006b; Zhang et al., 2008b,c). The present data and the spatial distribution of the Mesozoic igneous rocks do not favor either the mantle plume model or subduction of the Mongol–Okhotsk Ocean. Instead, subduction of the Paleo-Pacific plate is more consistent with the data (Zhang et al., 2008b and reference therein). The evidence supporting subduction of the Paleo-Pacific plate includes the occurrence of Jurassic accretionary complexes, tomographic studies and the spatial distribution of Mesozoic magmatism. Development of Jurassic accretionary complexes (Kojima, 1987; Natal'in, 1993; Isozaki, 1997; Maruyama, 1997; Wu et al., 2007a) and tomographic studies (Fukao et al., 1992; Huang and Zhao, 2006) clearly indicate that subduction of the Paleo-Pacific plate played an important role in the geodynamic evolution of eastern China and the whole of the Asian continental margin. Geochronological studies of the Heilongjiang Group, which is considered to be an accretionary complex, indicate Early Jurassic accretion and high-pressure metamorphism (Wu et al., 2007a; Zhou et al., 2009). Geophysical data also reveal a stagnant subducted slab at a depth of 660 km that forms a high velocity layer beneath eastern China, the western edge generally coinciding with a boundary of topographic change identified at the surface (Huang and Zhao, 2006). In addition, the linear distribution of Mesozoic igneous rocks along the eastern continental margin of China also implies a relationship between magmatism and subduction.

The question remains as to what deep geodynamic processes controlled the tectonic switch from compression to extension and the formation of the giant igneous events across the whole of eastern China. Taking the geological, geochronological and geophysical evidence together, an eastward migration of delamination associated with the subduction of the Paleo-Pacific plate is a possibility (Wang et al., 2006a,b). This process was probably accompanied by roll back of the subducted oceanic plate (Wu et al., 2007b), which steepened the subduction zone, as suggested by the geophysical studies (Huang and Zhao, 2006). Although timing of initiation of subduction of the Paleo-Pacific plate is not well constrained, it most likely occurred in the Jurassic. This process caused crustal shortening and thickening, resulted in widespread magmatism of active continental-margin affinity, and formed the westward younging trend of the granites, with only rare volcanic rocks. Subsequent delamination of the thickened eclogitic lower crust and underlying lithospheric mantle into the convecting asthenosphere would result in melting of the delaminated eclogites. Interaction of the resultant melt with peridotitic mantle would have formed the high-Mg adakitic magma (Gao et al., 2004). It has been suggested that delamination was relatively minor at this stage, whilst the major process was underplating of mantle-derived magma at the base of the lower crust and partial melting of pre-existing crust (Wu et al., 2005b). During this stage, the lithosphere was softened due to the addition of fluid released from the subducting slab, and magma extraction would facilitate delamination of the lower crust. At the end of the Jurassic, the westward flat subduction of the Paleo-Pacific plate beneath the Euro-Asian plate reached its peak and changed direction to the north or northwest (Maruyama et al., 1997; Sagong et al., 2005). This caused the change from compressional to extensional tectonics across the whole region, resulting in large-scale delamination of the thickened crust, elevation of the geotherm, and initiation of steep subduction. Delamination thus commenced at the western part of the subducted slab and migrated eastward. Delamination and consequent upwelling of the asthenosphere resulted in extensive magmatism (see Fig. 11). The eastward migration of delamination explains the observed younging trend of volcanism in this direction. The peak of delamination occurred at about 125 Ma, as manifested by the climax of magmatism (Wu et al., 2005a). The magmatic gap coincides with the transformation process from compression to extension, that is, the previously thickened crust started to delaminate extensively by the Early Cretaceous. The above subduction-induced delamination model can also be applied to other parts of eastern China, which were apparently also subjected to lithospheric thinning in the Mesozoic (Menzies et al., 1993; Menzies

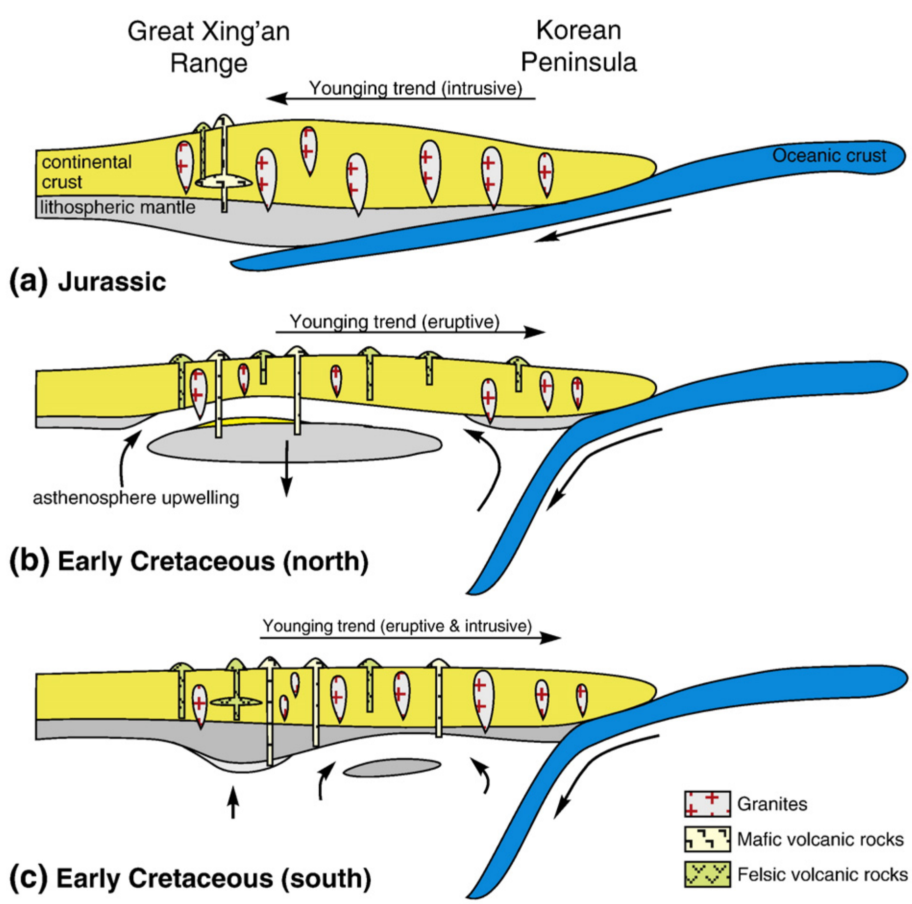

Fig. 11. Simplified cartoon depicting the subduction-induced delamination model. (a) Jurassic; (b) Early Cetaceous across the northern Great Xing'an Range; (c) Early Cretaceous across the southern Great Xing'an Range.

and Xu, 1998; Griffin et al., 1998; Wu and Sun, 1999; Wu et al., 2000c; Xu, 2001; Gao et al., 2002; Wu et al., 2003a,b; Gao et al., 2004;Wu et al., 2005a,b; Zhang, 2005; Wu et al., 2006; Zheng et al., 2006; Wu et al., 2008).

It is evident that although controlled by the same tectonic process, the geochronological framework of the volcanic rocks suggests that the northern and southern Great Xing'an Range reflect different deep lithospheric processes, as manifested in the rock assemblages, geochemistry and age of the volcanic rocks. This is reflected in the thermal state of the volcanic rocks. The calculated zircon saturation temperatures of the felsic rocks (Guo et al., 2008; unpul. data of the author) indicate that the magma temperatures have different trends in the northern and southern segments. In the northern segment, the temperatures increase significantly at the late stage of magmatism, while they actually decrease in the south, suggesting that during the late stage of volcanism, the northern Great Xing'an Range underwent a significant elevation of the geotherm relative to the southern segment (Guo et al., 2008). In the northern segment, elevation of the geotherm due to upwelling of the asthenosphere generated voluminous felsic rocks with low Ba and Sr concentrations, while in the southern segment, the significant temperature decrease meant that these felsic rocks were probably generated by fractionation within a relatively thick crust, explaining the sub-alkali trend (Fig. 4b). This conclusion is also supported by tomography studies, which indicate that the depth of the lithosphere–asthenosphere boundary in the southern Great Xing'an Range is significantly greater than that in adjacent regions (Huang and Zhao, 2006; Tang and Chen, 2008).

Based on the age framework and geochemistry, a broad subduction-induced migrating delamination model for the volcanic rocks in the Great Xing'an Range is proposed as follows (Fig. 11):

1) During the Jurassic, rapid flat subduction of the Paleo-Pacific plate beneath NE China resulted in the emplacement of voluminous granites of active continental-margin affinity and consequent thickening of the crust. Magmatic emplacement migrated westward with time as the subduction zone evolved (Fig. 11a). Underplated magma accumulated at the base of the crust and induced partial melting of pre-existing crustal materials, accompanied by local delamination of the thickened crust (Fig. 11a). At the end of the Jurassic, a change in the subduction direction led to a switch in the regional tectonic setting from compression to extension.
2) At the beginning of the Early Cretaceous, the thickened crust delaminated and induced regional extension. Delamination migrated from west to east, related to upwelling of asthenospheric mantle, elevation of the geotherm, and roll back and steepening of the subducting oceanic slab (Fig. 11b). However, delamination was not uniform across the area and was mainly restricted to the northern segment of the Great Xing'an Range and adjacent regions in northeastern China (O'Reilly et al., 2001). The lithospheric mantle, and even part of the lower crust, were delaminated and resulted in eruption of voluminous felsic magmas (Fig. 11b). However, in the southern Great Xing'an Range, delamination was not as significant as in the northern segment. Instead, underplating was predominant (Fig. 11c), which induced deepening of the lithosphere–asthenosphere boundary, as revealed by geophysical studies (Huang and Zhao, 2006; Tang and Chen, 2008).

7. Conclusions

1) A systematic geochronological study of the volcanic rocks in the southern Great Xing'an Range indicates that they were erupted in the Late Jurassic and Early Cretaceous, ranging in age from 174 Ma to 122 Ma. However, they are dominantly Early Cretaceous in age. The age data indicate that the previously-defined stratigraphic sequence is incorrect and needs to be revised.
2) Compilation of the age data indicates that two episodes of magmatism can be recognized in the Great Xing'an Range and can be related to a similar sequence of events identified in adjacent regions of NE China. There is a magmatic gap between Jurassic and Cretaceous volcanism, which increases in duration eastward to the continental margin and corresponds to the switch in the tectonic setting from compression to extension.
3) During the Late Jurassic, subduction of the Paleo-Pacific plate underneath the Eurasian continent resulted in thickening of the crust and generation of magmas of active continental-margin affinity, as accompanied by local delamination. During the Early Cretaceous, delamination reached its peak, causing voluminous magmatism across the whole of NE China and adjacent regions. The eastward migration of delamination triggered lithospheric thinning in eastern China and culminated in the giant igneous events in the Cretaceous.

Acknowledgments

We are grateful to Hong-Lin Yuan, Xiao-Ming Liu, Hu-Jun Gong and Chun-Rong Diwu at the State Key Laboratory of Continental Dynamics (Northwest University, Xi'an); Yong-Sheng Liu, Zhao-Chu Hu and Hai-Hong Chen at the State Key Laboratory of Geological Processes and Mineral Resources (China University of Geosciences, Wuhan); as well as Yu-Guang Ma and Qian Mao at the Institute of Geology and Geophysics, Chinese Academy of Sciences, for their assistance during the analyses. We are grateful to R. Rudnick, B. Natal'in, and F. Guo for their constructive comments on the manuscript. This work was financially supported by the National Natural Science Foundation of China (Grants 90714010, 40821061, 98014003, and 40634019), the Ministry of Education of China (B07039) and the MOST special funds from the State Key Laboratory of Continental Dynamics and the State Key Laboratory of Geological Processes and Mineral Resources.

Appendix A. Supplementary data

Supplementary data associated with this article can be found, in the online version, at doi:10.1016/j.chemgeo.2010.05.013.

References

Andersen, T., 2003. Correction of common lead in U–Pb analyses that do not report ^{204}Pb. Chemical Geology 192, 59–79.
Ballard, J.R., Palin, J.M., Williams, I.S., Campbell, I.H., Faunes, A., 2001. Two ages of porphyry intrusion resolved for the super-giant Chuquicamata copper deposit of northern Chile by ELA-ICP-MS and SHRIMP. Geology 29, 383–386.
Bird, P., 1979. Continental delamination and the Colorado Plateau. Journal of Geophysical Research 84, 7561–7571.
Black, L.P., Kamo, S.L., Allen, C.M., Davis, D.W., Aleinikoff, J.N., Wallay, J.W., Mundil, R., Campbell, I.H., Korsch, R.J., Williams, I.S., Foudoulis, C., 2004. Improved ^{206}Pb/^{238}U microprobe geochronology by the monitoring of a trace-element-related matrix effect: SHRIMP, ID-TIMS, ELA-ICP-MS and oxygen isotope documentation for a series of zircon standards. Chemical Geology 206, 115–140.
Chen, B., Jahn, B.M., Wilde, S.A., Xu, B., 2000. Two contrasting Paleozoic magmatic belts in northern Inner Mongolia, China: petrogenesis and tectonic implications. Tectonophysics 328, 157–182.
Chen, B., Tian, W.B., Zhai, M.G., Arakawa, Y., 2005. Zircon U–Pb geochronology and geochemistry of the Mesozoic magmatism in the Taihang Mountains and other places of the North China craton with implications for petrogenesis and geodynamic setting. Acta Petrologica Sinica 21, 13–24 (in Chinese with English abstract).
Chen, Z.G., Zhang, L.C., Zhou, X.H., Wan, B., Ying, J.F., Wang, F., 2006. Geochronology and geochemical characteristics of volcanic rocks section in Manzhouli Xinyouqi, Inner-Mongolia. Acta Petrologica Sinica 22, 2971–2986 (in Chinese with English abstract).
Chen, Z.G., Zhang, L.C., Zhou, X.H., Liu, Q., Wan, B., Wu, H.Y., 2007. Geochemical and geochronological characteristics of the Mesozoic volcanics in the northern margin of the Erlian Basin, Inner Mongolia. Abstracts of 2007 national meeting of the petrology, geodynamics and chemical geodynamics in China, pp. 260–262 (in Chinese).
Cheng, R.Y., Wu, F.Y., Ge, W.C., Sun, D.Y., Liu, X.M., Yang, J.H., 2006. Emplacement age of the Raohe Complex in eastern Heilongjiang Province and the tectonic evolution of

the eastern part of Northeastern China. Acta Petrologica Sinica 22, 353–376 (in Chinese with English abstract).
Davis, G.A., Zheng, Y.D., Wang, C., Darby, B.J., Zhang, C.H., Gehrels, G., 2001. Mesozoic tectonic evolution of the Yanshan fold and thrust belt, with emphasis on Hebei and Liaoning Provinces, northern China. In: Hendrix, M.S., Davies, G.A. (Eds.), Paleozoic and Mesozoic tectonic evolution of central Asia: From continental assembly to intracontinental deformation: GSA Memoir, 194, pp. 171–198.
Deng, J.F., Zhao, H.L., Mo, X.X., Luo, Z.H., Du, S.Y., 1996. Continental root/plume structure in China — key to the continental geodynamics. Geological Publishing House, Beijing, pp. 1–110.
Deng, J.F., Su, S.G., Liu, C., Zhao, G.C., Zhao, X.G., Zhou, S., Wu, Z.X., 2006. Discussion on the lithospheric thinning of the North China craton: delamination? or thermal erosion and chemical metasomatism? Earth Science Frontiers 13, 105–199 (in Chinese with English abstract).
Deng, J.F., Su, S.G., Niu, Y.L., Liu, C., Zhao, G.C., Zhao, X.G., Zhou, S., Wu, Z.X., 2007. A possible model for the lithospheric thinning of North China Craton: evidence from the Yanshanian (Jura-Cretaceous) magmatism and tectonism. Lithos 96, 22–35.
Ding, R.X., Shu, P., Ji, X.Y., Qu, Y.M., Chen, R.H., Zhang, B., 2007. SHRIMP zircon U–Pb age and geological meaning of reservoir volcanic rocks in Qingshen gas field of the Songliao Basin, NE China. Journal of Jilin University (Earth Science Edition) 37, 525–530 (in Chinese with English abstract).
Donskaya, T.V., Windley, B.F., Mazukabzov, A.M., Kröner, A., Sklyarov, E.V., Gladkochub, D.P., Ponomarchuk, V.A., Badarch, G., Reichow, M.K., Hegner, E., 2008. Age and evolution of late Mesozoic metamorphic core complexes in southern Siberia and northern Mongolia. Journal of the Geological Society of London 165, 405–421.
Fan, W.M., Guo, F., Wang, Y.J., Lin, G., 2003. Late Mesozoic calc-alkaline volcanism of post-orogenic extension in the northern Da Hinggan Mountains, Northeastern China. Journal of Volcanology and Geothermal Reseach 121, 115–135.
Fan, W.M., Guo, F., Gao, X.F., Li, C.W., 2008. Sr–Nd isotope mapping of Mesozoic igneous rocks in NE China: constraints on tectonic framework and crustal growth. Geochemica 37, 361–372 (in Chinese with English abstract).
Fukao, Y., Obayashi, M., Inoue, H., Nenbai, M., 1992. Subducting slabs stagnant in the mantle transition zone. Journal of Geophysical Research 97, 4809–4822.
Gao, Y., 2008. Chronology and Geochemistry of Mesozoic Volcanic Rocks in Southeastern Songliao Basin. Master Dissertation, Jilin University, 1–78.
Gao, S., Luo, T.C., Zhang, B.R., Zhang, H.F., Han, Y.W., Hu, Y.K., Zhao, Z.D., 1998a. Chemical composition of the continental crust as revealed by studies in East China. Geochimica et Cosmochimica Acta 62, 1959–1975.
Gao, S., Zhang, B.R., Jin, Z.M., Kern, H., Luo, T.C., Zhao, Z.D., 1998b. How mafic is the lower continental crust? Earth and Planetary Science Letters 161, 101–117.
Gao, S., Rudnick, R.L., Carlson, R.W., McDonough, W.F., Liu, Y.S., 2002. Re–Os evidence for replacement of ancient mantle lithosphere beneath the North China Craton. Earth and Planetary Science Letters 198, 307–322.
Gao, S., Rudnick, R.L., Yuan, H.L., Liu, X.M., Liu, Y.S., Xu, W.L., Ling, W.L., Ayers, J., Wang, X.C., Wang, Q.H., 2004. Recycling lower continental crust in the North China Craton. Nature 432, 892–897.
Gao, X.F., Guo, F., Fan, W.M., Li, C.W., Li, X.Y., 2005. Origin of Late Mesozoic intermediate-felsic volcanic rocks from the southern Da Hinggan Mountain, NE China. Acta Petrologica Sinica 21, 737–748 (in Chinese with English abstract).
Gao, F.H., Xu, W.L., Yang, D.B., Pei, F.P., Liu, X.M., Hu, Z.C., 2007. LA-ICP-MS zircon U–Pb dating from granitoids in southern basement of Songliao basin: constraints on ages of the basin basement. Science in China (Serises D) 50, 995–1004.
Ge, W.C., Lin, Q., Sun, D.Y., Wu, F.Y., Won, C.K., Lee, M.W., Jin, M.S., Yun, S.H., 1999. Geochemical characteristics of the Mesozoic basalts in Da Hinggan Ling: Evidence of the mantle–crust interaction. Acta Petrologica Sinica 15, 397–407 (in Chinese with English abstract).
Ge, W.C., Lin, Q., Sun, D.Y., Wu, F.Y., Li, X.H., 2000a. Geochemical research into origins of two types of Mesozoic rhyolites in Daxing'an Ling. Earth Science-Journal of China University of Geosciences 36, 172–178 (in Chinese with English abstract).
Ge, W.C., Lin, Q., Li, X.H., Sun, D.Y., Wu, F.Y., 2000b. Geochemical characteristics of basalts of the Early Cretaceous Yiliekede Formation, North Daxing'an Ling. Journal of Mineralogy and Petrology 20, 14–18 (in Chinese with English abstract).
Ge, W.C., Li, X.H., Lin, Q., Sun, D.Y., Wu, F.Y., Yun, S.H., 2001. Geochemistry of early Cretaceous alkaline rhyolites from Hulun Lake, Da Xing'an Ling and its tectonic implication. Chinese Journal of Geology 36, 176–183 (in Chinese with English abstract).
Ge, W.C., Wu, F.Y., Zhou, C.Y., Abdel Rahman, A.A., 2005a. Emplacement age of the Tahe granite and its constraints on the tectonic nature of the Eguna block in the northern part of the Great Xing'an Range. Chinese Science Bulletin 50, 2097–2105.
Ge, W.C., Wu, F.Y., Zhou, C.Y., Zhang, J.H., 2005b. Zircon U–Pb ages and its significance of the Mesozoic granites in the Wulanhaote Region, central Great Xing'an Range. Acta Petrologica Sinica 21, 749–762 (in Chinese with English abstract).
Ge, W.C., Sui, Z.M., Wu, F.Y., Zhang, J.H., Xu, X.C., Cheng, R.Y., 2007a. Zircon U–Pb ages, Hf isotopic characteristics and their implications of the Early Paleozoic granites in the northeastern Da Hinggan Mts., northeastern China. Acta Petrologica Sinica 23, 423–440 (in Chinese with English abstract).
Ge, W.C., Wu, F.Y., Zhou, C.Y., Zhang, J.H., 2007b. Porphyry Cu–Mo deposits in the eastern Xing'an–Mongolian Orogenic Belt: mineralization ages and their geodynamic implications. Chinese Science Bulletin 52, 3416–3427.
Griffin, W.L., Zhang, A.D., O'Reilly, S.Y., Ryan, C.G., 1998. Phanerozoic evolution of the lithosphere beneath the Sino-Korean craton. In: Flower, M.F.J., Chung, S.L., Lo, C.H., Lee, T.Y. (Eds.), In Mantle Dynamics and Plate Interactions in East Asia. Geodynamic Series, 27. American Geophysical Union, Washington, D. C, pp. 107–126.
Guo, F., Fan, W.M., Wang, Y.J., Lin, G., 2001. Petrogenesis of the late Mesozoic bimodal volcanic rocks in the southern Da Hinggan Mts., China. Acta Petrologica Sinica 17, 161–168 (in Chinese with English abstract).
Guo, F., Fan, W.M., Li, C.W., Gao, X.F., Miao, L.C., 2008. Early Cretaceous highly positive ε_{Nd} felsic volcanic rocks from the Hinggan Mountains, NE China: origin and implications for Phanerozoic crustal growth. International Journal of Earth Sciences. doi:10.1007/s00531-008-0362-8.
HBGMR (Hebei Bureau of Geology and Mineral Resources), 1989. Regional geology of Hebei Province, Beijing Municipality and Tianjin Municipality. Geological Publishing House, Beijing, pp. 1–741 (in Chinese with English abstract).
HBGMR (Heilongjiang Bureau of Geology Mineral Resources), 1993. Regional geology of Heilongjiang Province. Geological Publishing House, Beijing, pp. 1–734 (in Chinese with English abstract).
Hong, D.W., Huang, H.Z., Xiao, Y.J., Xu, H.M., Jin, M.Y., 1994. The Permian alkaline granites in central Inner Mongolia and the geodynamic significance. Acta Geologica Sinica 68, 219–230 (Chinese edition, in Chinese with English abstract).
Horn, I., Rudnick, R.L., McDonough, W.F., 2000. Precise elemental and isotope ratio determination by simultaneous solution nebulization and laser ablation-ICP-MS: application to U–Pb geochronology. Chemical Geology 167, 405–425.
Huang, J.L., Zhao, D.P., 2006. High-resolution mantle tomography of China and Surrounding regions. Journal of Geophysical Research 111, B09305. doi:10.1029/2005JB004066.
IMBGMR (Inner Mongolia Bureau of Geology Mineral Resources), 1991. Regional Geology of Inner Mongolia. Geological Publishing House, Beijing, pp. 1–725 (in Chinese with English abstract).
Irvine, T.N., Baragar, W.R.A., 1971. A guide to the chemical classification of the common volcanic rocks. Canadian Journal of Earth Sciences 8, 523–548.
Isozaki, Y., 1997. Jurassic accretion tectonics of Japan. The Island Arc 6, 25–51.
Jackson, S.E., Pearson, N.J., Griffin, W.L., Belousova, E.A., 2004. The application of laser ablation-inductively coupled plasma-mass spectrometry to in situ U–Pb zircon geochronology. Chemical Geology 211, 47–69.
Jahn, B.M., 2004. The Central Asian Orogenic Belt and growth of the continental crust in the Phanerozoic. In: Malpas, J., Fletcher, C.J.N., Ali, J.R., Aitchison, J.C. (Eds.), Aspects of the Tectonic Evolution of China. Special Publication, 226. Geological Society of London, pp. 73–100.
Jahn, B.M., Wu, F.Y., Chen, B., 2000. Massive granitoids generation in central Asia: Nd isotopic evidence and implication for continental growth in the Phanerozoic. Episodes 23, 82–92.
Jahn, B.M., Wu, F.Y., Capdevila, R., Martineau, F., Zhao, Z.H., Wang, Y.X., 2001. Highly evolved juvenile granites with tetrad REE patterns: the Woduhe and Baerzhe granites from the Great Xing'an Mountains in NE China. Lithos 59, 171–198.
Ji, W.Q., 2007. Chronology and geochemistry of Late Mesozoic volcanic rocks in eastern Jilin and Heilongjiang Provinces. Masters Dissertation, Jilin University, 64pp.
Ji, W.Q., Xu, W.L., Yang, D.B., Pei, F.P., 2005. Forming time of the Mesozoic volcanic rocks in the eastern Heilongjiang Province. Bulletin of Mineralogy, Petrology and Geochemistry 24 suppl., 120 (in Chinese).
Jiang, G.Y., Quan, H., 1988. Mesozoic volcanic rocks of Genhe and Hailar basins in Da Hinggan Ling Range. Bulletin of Shenyang Institute Research, Chinese Academy of Geological Science 17, 23–100 (in Chinese with English abstract).
Kay, R.W., Kay, S.M., 1993. Delamination and delamination magmatism. Tectonophysics 219, 177–189.
Kinoshita, O., 1995. Migration of igneous activities related to ridge subduction on Southwest Japan and the East Asian continental margin from the Mesozoic to the Paleogene. Tectonophysics 245, 25–35.
Kojima, S., 1987. Mesozoic terrane accretion in northeast China, Sikhote-Alin and Japan regions. Palaeogeography, Palaeoclimatology, Palaeoecology 69, 213–232.
Košler, J., Fonneland, H., Sylvester, P., Tubrett, M., Pedersen, R.B., 2002. U–Pb dating of detrital zircons for sediment provenance studies — a comparison of laser ablation ICPMS and SIMS techniques. Chemical Geology 182, 605–618.
Li, R.S., 1991. Xinlin ophiolite. Heilongjiang Geology 2, 19–32 (in Chinese with English abstract).
Li, J.Y., 2006b. Permian geodynamic setting of Northeast China and adjacent regions: closure of the Paleo-Asian Ocean and subduction of the Paleo-Pacific Plate. Journal of Asian Earth Sciences 26, 207–224.
Li, C.W., 2006a. Petrogenesis and geological implications of the late Mesozoic volcanic rocks in southeastern Jilin Province, northeastern China. Ph. D. Dissertation, Graduate School of The Chinese Academy of sciences, 121pp.
Li, P.Z., Yu, J.S., 1993. Nianzishan miarolitic alkaline granite stock. Heilongjiang: its age and geological implications. Geochimica 4, 389–398 (in Chinese with English abstract).
Li, H.M., Dong, C.W., Xu, X.S., Zhou, X.M., 1995. The single grain zircon U–Pb age of the Quanzhou gabbro — the source of mafic igneous rock in Southeast Fujian Province. Chinese Science Bulletin 40, 158–160 (in Chinese).
Li, X.H., Liang, X.R., Sun, M., Liu, Y., Tu, X., 2000. Geochronology and geochemistry of single-grain zircons: simultaneously in-situ analysis of U–Pb age and trace elements by LAM-ICP-MS. European Journal of Mineralogy 12, 1015–1024.
Li, X.H., Liang, X.R., Sun, M., Guan, H., Malpas, J.G., 2001. Precise ^{206}Pb–^{238}U age determination on zircons by laser ablation microprobe-inductively coupled plasma-mass spectrometry using continuous linear ablation. Chemical Geology 175, 209–219.
Li, C.W., Guo, F., Fan, W.M., Gao, X.F., 2007. Ar–Ar geochronology of Late Mesozoic volcanic rocks from the Yanji area, NE China and tectonic implications. Science in China (Series D) 50, 505–518.
Lin, W., Wang, Q.C., 2006. Late Mesozoic extensional tectonics in the North China block: a crustal response to subcontinental mantle removal? Bulletin of Society Géologie France 177, 287–297.

Lin, Q., Ge, W.C., Sun, D.Y., Wu, F.Y., Won, C.K., Min, K.D., Jin, M.S., Lee, M.W., Kwon, C.S., Yun, S.H., 1998. Tectonic implications of Mesozoic volcanic rocks in Northeastern China. Scientia Geologica Sinica 33, 129–139 (in Chinese with English abstract).

Lin, Q., Ge, W.C., Sun, D.Y., Wu, F.Y., Won, C.K., Lee, M.W., Yun, S.H., Jin, M.S., Min, K.D., Kwon, C.S., 2000. Genetic relationships between two types of Mesozoic rhyolite and basalts in Great Xing'an Range. Journal of Changchun University of Science and Technology 30, 322–328.

Lin, Q., Ge, W.C., Cao, L., Sun, D.Y., Lim, K.G., 2003. Geochemistry of Mesozoic volcanic rocks in Da Hinggan Ling: the bimodal volcanic rocks. Geochimica 32, 208–222 (in Chinese with English abstract).

Lin, Q., Ge, W.C., Wu, F.Y., Sun, D.Y., Cao, L., 2004. Geochemistry of Mesozoic granites in Da Hinggan Ling ranges. Acta Petrologica Sinica 20, 403–412 (in Chinese with English abstract).

Liu, J.L., Davis, G.A., Lin, Z.Y., Wu, F.Y., 2005a. The Liaonan metamorphic core complex, Southeastern Liaoning Province, North China: a likely contributor to Cretaceous rotation of Eastern Liaoning, Korea and contiguous areas. Tectonophysics 407, 65–80.

Liu, W., Siebel, T.W., Li, X., Pan, X., 2005b. Petrogenesis of the Linxi granitoids, northern Inner Mongolia of China: constraints on basaltic underplating. Chemical Geology 219, 5–35.

Liu, X.M., Gao, S., Diwu, C.R., Yuan, H.L., Hu, Z.C., 2007. Simultaneous *in situ* determination of U–Pb age and trace elements in zircon by LA-ICP-MS in 20 μm spot size. Chinese Science Bulletin 52, 1257–1264.

Liu, Y.S., Hu, Z.C., Zong, K.Q., Gao, C.G., Gao, S., Xu, J., Chen, H.H., 2010. Reappraisement and refinement of zircon U-Pb isotope and trace element analyses by LA-ICP-MS. Chinese Science Bulletin 55, 1535–1546.

Ludwig, K.R., 2003. Isoplot 3.0 — a geochronological toolkit for Microsoft Excel. Special Publication, 4. Berkeley Geochronology Center (70 pp.).

Lustrino, M., 2005. How the delamination and detachment of lower crust can influence basaltic magmatism. Earth Science Reviews 72, 21–38.

Maruyama, S., 1997. Pacific-type orogeny revisited: Miyashiro-type orogeny proposed. The Island Arc 6, 91–120.

Maruyama, S., Isozaki, Y., Kimura, G., Terabayashi, M., 1997. Paleogeographic maps of the Japanese Islands: plate tectonic synthesis from 750 Ma to the present. The Island Arc 6, 121–142.

Meng, Q.R., 2003. What drove late Mesozoic extension of the northern China — Mongolia tract? Tectonophysics 369, 155–174.

Menzies, M.A., Xu, Y.G., 1998. Geodynamics of the North China craton. In: Flower, M.F.J., Chung, S.L., Lo, C.H., Lee, T.Y. (Eds.), Mantle Dynamics and Plate Interactions in East Asia. Geodynamic Series, 100. American Geophysical Union, Washington, D.C, pp. 155–165.

Menzies, M.A., Fan, W.M., Zhang, M., 1993. Paleozoic and Cenozoic lithoprobe and the loss of >120 km of Archean lithosphere, Sino-Korean craton, China. In: Prichard, H.M., Alabaster, T., Harris, N.B.W., Neary, C.R. (Eds.), Magmatic Processes and Plate Tectonic. Special Publication, 76. Geological Society, pp. 71–81.

Miao, L.C., Fan, W.M., Zhang, F.Q., Liu, D.Y., Jian, P., Shi, G.H., Tao, H., Shi, Y.R., 2004. Zircon SHRIMP geochronology of the Xinkailing–Kele complex in the northwestern Lesser Xing'an Range, and its geological implications. Chinese Science Bulletin 49, 201–209.

Miao, L.C., Liu, D.Y., Zhang, F.Q., Fan, W.M., Shi, Y.R., Xie, H.Q., 2007. Zircon SHRIMP U–Pb ages of the “Xinghuadukou Group” in Hanjiayuanzi and Xinlin areas and the “Zhalantun Group” in Inner Mongolia, Da Hinggan Mountains. Chinese Science Bulletin 52, 1112–1134.

Natal'in, B.A., 1993. History and modes of Mesozoic accretion in southeastern Russia. The Island Arc 2, 15–34.

O'Reilly, S.Y., Griffin, W.L., Poudjom Djomani, Y.H., Morgan, P., 2001. Are Lithospheres Forever? Tracking changes in subcontinental lithospheric mantle through time. GSA Today 11 (4), 4–10.

Paul, B., Woodhead, J.D., Hergt, J., 2005. Improved in situ isotope analysis of low-Pb materials using LA-MC-ICP-MS with parallel ion counter and Faraday detection. Journal of Analytical Atomic Spectrometry 20, 1350–1357.

Pei, F.P., Xu, W.L., Yang, D.B., Zhao, Q.G., Liu, X.M., Hu, Z.C., 2007. Zircon U–Pb geochronology of basement metamorphic rocks in the Songliao Basin. Chinese Science Bulletin 52, 942–948.

Qin, K.Z., Li, H.M., Li, W.S., Shunso, I., 1999. Intrusion and mineralization age of the Wunugetushan porphyry Cu–Mo deposit, Inner Mongolia, northwestern China. Geological Review 45, 181–185 (in Chinese with English abstract).

Robinson, P.T., Zhou, M.F., Hu, X.F., Reynolds, P., Bai, W.J., 1999. Geochemical constraints on the petrogenesis and tectonic setting of the Hegenshan ophiolite, Northern China. Journal of Asian Earth Sciences 17, 423–442.

Sagong, H., Kwon, S.T., Ree, J.H., 2005. Mesozoic episodic magmatism in South Korea and its tectonic implication. Tectonics 24 (2004TC001720).

Sengör, A.M.C., Natal'in, B.A., Burtman, V.S., 1993. Evolution of the Altaid tectonic collage and Palaeozoic crustal growth in Eurasia. Nature 364, 299–307.

Shao, J.A., Zhang, L.Q., 2002. Mesozoic dyke swarms in the north of Northern China. Acta Petrologica Sinica 18, 312–318 (in Chinese with English abstract).

Shao, J.A., Zang, S.X., Mo, B.L., Li, X.B., Wang, B., 1995. Extension of orogenic belts and upwelling of ansthenosphere: the example of Hinggan–Mongolian orogenic belt. Chinese Science Bulletin 40, 50–56.

Shao, J.A., Zhang, L.Q., Mou, B.L., 1998. Thermo-tectonic evolution in middle and south part of Dahinggan. Science in China (Series D) 28, 194–200 (in Chinese).

Shao, J.A., Han, Q.J., Zhang, L.Q., Mu, B.L., Qiao, G.S., 1999. Two kinds of vertical accretion of the continental crust: an example of the Da Hinggan Mts. Acta Petrologica Sinica 15, 600–605 (in Chinese with English abstract).

Shao, J.A., Li, X.H., Zhang, L.Q., Mu, B.L., Liu, Y.L., 2001a. Geochemical conditions for genetic mechanism of the Mesozoic bimodal dyke swarms in Nankou-Guyaju. Geochemica 30, 517–524 (in Chinese with English Abstract).

Shao, J.A., Liu, F.T., Chen, H., Han, Q.J., 2001b. Relationship between Mesozoic magmatism and subduction in Da Hinggan–Yanshan area. Acta Geologica Sinica 75, 56–63 (in Chinese with English abstract).

Shi, G.H., Miao, L.C., Zhang, F.Q., Jian, P., Fan, W.M., Liu, D.Y., 2004. Emplacement age and tectonic implications of Xilinhot A-type granite in Inner Mongolia, China. Chinese Science Bulletin 49, 723–729.

Shu, P., Ding, R.X., Ji, X.Y., Qu, Y.M., 2007. SHRIMP zircon geochronology of reservoir volcanic rocks in the Qingshen gas field, Songliao Basin. Acta Petrologica et Mineralogica 26, 239–246 (in Chinese with English abstract).

Sui, Z.M., Ge, W.C., Wu, F.Y., Zhang, J.H., Xu, X.C., Cheng, R.Y., 2007. Zircon U–Pb ages, geochemistry and its petrogenesis of Jurassic granites in northeastern part of the Da Hinggan Mts. Acta Petrologica Sinica 23, 461–480 (in Chinese with English abstract).

Sun, D.Y., 2001. Petrogenesis and geodynamic significance of the Mesozoic granites in the Zhangguangcai Range. Ph. D. Dissertation, Jilin University. 96pp.

Sun, D.Y., Wu, F.Y., Li, H.M., Lin, Q., 2001a. Emplacement age of the postorogenic A-type granites in Northwestern Lesser Xing'an Ranges, and its relationship to the eastward extension of Suolunshan–Hegenshan–Zhalaite collisional suture zone. Chinese Science Bulletin 46, 427–432.

Sun, D.Y., Wu, F.Y., Lin, Q., Lu, X.P., 2001b. Petrogenesis and crust–mantle interaction of early Yanshanian Baishishan pluton in Zhangguangcai Range. Acta Petrologica Sinica 17, 227–235 (in Chinese with English abstract).

Sun, D.Y., Wu, F.Y., Gao, S., Lu, X.P., 2005a. Confirmation of two episodes of A-type granite emplacement during Late Triassic and Early Jurassic in the central Jilin Province, and their constraints on the structural pattern of Eastern Jilin–Heilongjiang Area, China. Earth Science Frontiers 12, 263–275 (in Chinese with English abstract).

Sun, D.Y., Suzuki, K., Wu, F.Y., Lu, X.P., 2005b. CHIME dating and its application for Mesozoic granites of Huanggoushan, Jilin Province. Geochimica 34, 305–314 (in Chinese with English abstract).

Tang, K.D., 1990. Tectonic development of Paleozoic fold belts at the north margin of the Sino-Korean craton. Tectonics 9, 249–260.

Tang, Q.S., Chen, L., 2008. Structure of the crust and uppermost mantle of the Yanshan Belt and adjacent regions at the northeastern boundary of the North China Craton from Rayleigh Wave Dispersion Analysis. Tectonophysics 455, 43–52.

Wang, X.G., Wang, Y., 2007. SHRIMP U–Pb dating of igneous rocks from the basement of north belt of the south Songliao Basin and its geological significance. Geological Science Technology Information 26, 23–27 (in Chinese with English abstract).

Wang, Y.X., Zhao, Z.H., 1997. Geochemistry and origin of the Baerzhe REE–Nb–Be–Zr super-large deposit. Geochimica 26, 24–35 (in Chinese with English abstract).

Wang, Y.Q., Su, Y.Z., Liu, E.Y., 1997. Regional strata of northeast China. China University of Geosciences Publishing House, Wuhan, pp. 1–175 (in Chinese).

Wang, P.J., Liu, Z.J., Wang, S.X., Song, W.H., 2002. $^{40}Ar/^{39}Ar$ and K/Ar dating of the volcanic rocks in the Songliao basin, NE China: constraints on stratigraphy and basin dynamics. International Journal of Earth Sciences 91, 331–340.

Wang, F., He, H.Y., Zhu, R.X., Sang, H.Q., Wang, Y.L., Yang, L.K., 2005. Intercalibration of international and domestic $^{40}Ar/^{39}Ar$ dating standards. Science in China (Series D) 49, 461–470.

Wang, F., Zhou, X.H., Zhang, L.C., Ying, J.F., Zhang, Y.T., Wu, F.Y., Zhu, R.X., 2006b. Late Mesozoic volcanism in the Great Xing'an Range (NE China): timing and implications for the dynamic setting of NE Asia. Earth and Planetary Science Letters 251, 179–198.

Wang, Y., Zhang, F.Q., Zhang, D.W., Miao, L.C., Li, T.S., Xie, H.Q., Meng, Q.R., Liu, D.Y., 2006a. Zircon SHRIMP U–Pb dating of meta-diorite from the basement of the Songliao Basin and its geological significance. Chinese Science Bulletin 51, 1877–1883.

Wilde, S.A., Dorsett-Bain, H.L., Liu, J.L., 1997. The identification of a Late Pan-African granulite facies event in Northeastern China: SHRIMP U–Pb zircon dating of the Mashan Group at Liu Mao, Heilongjiang Province, China. Proceedings of the 30th IGC: Precambrian Geology and Metamorphic Petrology, VSP International, 17. Science Publishers, Amsterdam, pp. 59–74.

Wilde, S.A., Zhang, X.Z., Wu, F.Y., 2000. Extension of a newly-identified 500 Ma metamorphic terrain in Northeast China: Further U–Pb SHRIMP dating of the Mashan Complex, Heilongjiang Province, China. Tectonophysics 328, 115–130.

Wilde, S.A., Wu, F.Y., Zhang, X.Z., 2003. Late Pan-African magmatism in Northeastern China: SHRIMP U–Pb zircon evidence for igneous ages from the Mashan Complex. Precambrian Research 122, 311–327.

Wu, F.Y., Sun, D.Y., 1999. The Mesozoic magmatism and lithospheric thinning in Eastern China. Journal of Changchun University of Science and Technology 29, 313–318 (in Chinese with English abstract).

Wu, F.Y., Lin, Q., Ge, W.C., Sun, D.Y., 1998. The petrogenesis and age of Xinhuatun pluton in Zhangguangcailing. Acta Petrologica et Mineralogica 17, 226–234 (in Chinese with English abstract).

Wu, F.Y., Jahn, B.M., Wilde, S.A., Sun, D.Y., 2000a. Phanerozoic continental crustal growth: U–Pb and Sr–Nd isotopic evidence from the granites in northeastern China. Tectonophysics 328, 89–113.

Wu, F.Y., Sun, D.Y., Li, H.M., Wang, X.L., 2000b. Zircon U–Pb ages of the basement rocks beneath the Songliao Basin, NE China. Chinese Science Bulletin 45, 1514–1518.

Wu, F.Y., Sun, D.Y., Zhang, G.L., Ren, X.W., 2000c. Deep geodynamics of Yanshan Movement. Geological Journal of China Universities 6, 379–388 (in Chinese with English abstract).

Wu, F.Y., Sun, D.Y., Li, H.M., Wang, X.L., 2001. The nature of basement beneath the Songliao Basin in NE China: geochemical and isotopic constraints. Physics and Chemistry of the Earth (Part A) 26, 793–803.

Wu, F.Y., Sun, D.Y., Li, H.M., Jahn, B.M., Wilde, S.A., 2002. A-type granites in northeastern China: age and geochemical constraints on their petrogenesis. Chemical Geology 187, 143–173.
Wu, F.Y., Ge, W.C., Sun, D.Y., Guo, C.L., 2003a. Discussions on the lithospheric thinning in Eastern China. Earth Science Frontiers 10, 51–59 (in Chinese with English abstract).
Wu, F.Y., Jahn, B.M., Wilde, S.A., Lo, C.H., Yui, T.F., Lin, Q., Ge, W.C., Sun, D.Y., 2003b. Highly fractionated I-type granites in NE China (II): isotopic geochemistry and implications for crustal growth in the Phanerozoic. Lithos 67, 191–204.
Wu, F.Y., Walker, R.J., Ren, X.W., Sun, D.Y., Zhou, X.H., 2003c. Osmium isotope constraints on the age of lithospheric mantle beneath the northeast China. Chemical Geology 197, 107–129.
Wu, F.Y., Sun, D.Y., Jahn, B.M., Wilde, S.A., 2004a. A Jurassic garnet-bearing granitic pluton from NE China showing tetrad REE patterns. Journal of Asian Earth Sciences 23, 731–744.
Wu, F.Y., Wilde, S.A., Sun, D.Y., Zhang, G.L., 2004b. Geochronology and petrogenesis of post-orogenic Cu, Ni-bearing mafic–ultramafic intrusions in Jilin, NE China. Journal of Asian Earth Sciences 23, 781–797.
Wu, F.Y., Lin, J.Q., Wilde, S.A., Zhang, X.O., Yang, J.H., 2005a. Nature and significance of the Early Cretaceous giant igneous event in eastern China. Earth and Planetary Science Letters 233, 103–119.
Wu, F.Y., Yang, J.H., Wilde, S.A., Zhang, X.O., 2005b. Geochronology, petrogenesis and tectonic implications of Jurassic granites in the Liaodong Peninsula, NE China. Chemical Geology 221, 127–156.
Wu, G., Sun, D.Y., Zhao, C.S., Li, Z.T., Zhao, A.L., Pang, Q.B., Li, G.Y., 2005c. Discovery of the Early Paleozoic post orogenic granite in northern margin of the Erguna massif and its significance. Chinese Science Bulletin 50, 2733–2743.
Wu, G., Zhu, Q., Li, Z.D., Wang, X.J., Wang, H.B., Li, G.Y., Pang, Q.B., 2005d. Geochemical feature and $^{40}Ar/^{39}Ar$ dating of the Mesozoic volcanic rocks in the northern Great Xing'an Range. Abstract of 2005 national meeting of the petrology and geodynamics in China, pp. 127–130 (in Chinese).
Wu, F.Y., Walker, R.J., Yang, Y.H., Yuan, H.L., Yang, J.H., 2006. The chemical–temporal evolution of lithospheric mantle underlying the North China Craton. Geochimica et Cosmochimica Acta 70, 5013–5034.
Wu, F.Y., Yang, J.H., Lo, C.H., Wilde, S.A., Sun, D.Y., Jahn, B.M., 2007a. The Jiamusi Massif: a Jurassic accretionary terrane along the western Pacific margin of NE China. The Island Arc 16, 156–172.
Wu, F.Y., Han, R.H., Yang, J.H., Wilde, S.A., Zhai, M.G., Park, S.C., 2007b. Initial constraints on the timing of granitic magmatism in North Korea using U–Pb zircon geochronology. Chemical Geology 238, 232–248.
Wu, F.Y., Xu, Y.G., Gao, S., Zheng, J.P., 2008. Controversial on studies of the lithospheric thinning and craton destruction of North China. Acta Petrologica Sinica 24, 1145–1174 (in Chinese with English abstract).
Xu, Y.G., 2001. Thermo-tectonic destruction of the Archean lithospheric keel beneath eastern China: evidence, timing and mechanism. Physics and Chemistry of the Earth (A) 26, 747–757.
Xu, Y.G., 2006. Using basalt geochemistry to constrain Mesozoic–Cenozoic evolution of the lithosphere beneath North China Craton. Earth Science Frontiers 13, 93–104 (in Chinese with English abstract).
Xu, Y.G., Huang, X.L., Ma, J.L., Wang, Y.B., Iizuka, Y., Xu, J.F., Wang, Q., Wu, X.Y., 2004. Crust–mantle interaction during the tectono-thermal reactivation of the North China Craton: constraints from SHRIMP zircon U–Pb chronology and geochemistry of Mesozoic plutons from western Shandong. Contributions to Mineralogy and Petrolgy 147, 750–767.
Xu, W.L., Gao, S., Wang, Q.H., Wang, D.Y., Liu, Y.S., 2006. Mesozoic crustal thickening of the eastern North China Craton: evidence from eclogite xenoliths and petrologic implications. Geology 34, 721–724.
Xu, Y.G., Blusztajn, J., Ma, J.L., Suzuki, K., Liu, J.F., Hart, S.R., 2008a. Late Archean to Early Proterozoic lithospheric mantle beneath the western North China craton: Sr–Nd–Os isotopes of peridotite xenoliths from Yangyuan and Fansi. Lithos 102, 25–42.
Xu, W.L., Hergt, J.M., Gao, S., Pei, F.P., Wang, W., Yang, D.P., 2008b. Interaction of adakitic melt-peridotite: implications for the high-$Mg^{\#}$ signature of Mesozoic adakitic rocks in the eastern North China Craton. Earth and Planetary Science Letters 265, 123–137.
Xu, W.L., Pei, F.P., Gao, F.H., Yang, D.B., Bu, Y.J., 2008c. Zircon U–Pb age from basement granites in Yishu graben and its tectonic implications. Earth Science-Journal of China University of Geosciences 33, 145–150 (in Chinese with English abstract).
Yan, J.Y., Tang, K.D., Bai, J.W., Mo, Y.C., 1989. High pressure metamorphic rocks and their tectonic environment in northeastern China. Journal of Southeastern Asian Earth Sciences 3, 303–313.
Yang, Z.Z., Meng, Q.C., Gang, J., Han, X.P., 1996. Liaonan Metamorphic core complex. Liaoning Geology 4, 241–250 (in Chinese with English abstract).
Yang, J.H., Wu, F.Y., Chung, S.L., Lo, C.H., Wilde, S.A., Davis, G.A., 2007a. Rapid exhumation and cooling of the Liaonan metamorphic core complex: inferences from $^{40}Ar/^{39}Ar$ thermochronology and implications for Late Mesozoic extension in the eastern North China Craton. GSA Bulletin 119, 1405–1414.
Yang, J.H., Wu, F.Y., Liu, X.M., Xie, L.W., Yang, Y.H., 2007b. Petrogenesis and geological significance of the Jurassic Xiaoheishan Pluton in the Liaodong Peninsula, East China: in situ zircon U–Pb dating and Hf isotopic analysis. Bulletin of Mineralogy, Petrology and Geochemistry 26, 29–43 (in Chinese with English abstract).
Ye, H.W., Zhang, X.Z., Zhou, Y.W., 1994. The texture and evolution of Manzhouli-Suifenhe lithosphere-study based on features of blueschist and ophiolites. In: M-SGT geological project group (Ed.), Geological study on the texture and evolution of the Manzhouli–Suifenhe geological section in China. Seismic Publishing House, 73–83.
Yuan, H.L., Wu, F.Y., Gao, S., Liu, X.M., Xu, P., Sun, D.Y., 2003. Determination of U–Pb age and rare earth element concentrations of zircons from Cenozoic intrusions in northeastern China by laser ablation ICP-MS. Chinese Science Bulletin 48, 2411–2421.
Yuan, H.L., Gao, S., Liu, X.M., Li, H.M., Gunther, D., Wu, F.Y., 2004. Accurate U–Pb age and trace element determinations of zircon by laser ablation-inductively coupled plasma mass spectrometry. Geostandard Newsletters 28, 353–370.
Yuan, H.L., Gao, S., Dai, M.N., Zong, C.L., Günther, D., Fontaine, G.H., Liu, X.M., Diwu, C.R., 2008. Simultaneous determinations of U–Pb age, Hf isotopes and trace element compositions of zircon by excimer laser-ablation quadrupole and multiple-collector ICP-MS. Chemical Geology 247, 100–118.
Zhai, M.G., Meng, Q.R., Liu, J.M., Hou, Q.L., Hu, S.B., Li, Z., Zhang, H.F., Liu, W., Shao, J.A., Zhu, R.X., 2004. Geological features of Mesozoic tectonic regime inversion in Eastern North China and implication for geodynamics. Earth Science Frontiers 11, 285–297.
Zhang, H.F., 2005. Transformation of lithospheric mantle through peridotite-melt reaction: a case of Sino-Korean craton. Earth and Planetary Science Letters 237, 768–780.
Zhang, J.H., 2006. Geochronological framework of the Mesozoic volcanic rocks in the Great Xing'an Range, NE China. Master Dissertation, Jilin University, 1–94.
Zhang, Y.P., Tang, K.D., 1989. Pre-Jurassic tectonic evolution of intercontinental region and the suture zone between the North China and Siberian platforms. Journal of Southeast Asian Earth Sciences 3, 47–55.
Zhang, L.Q., Shao, J.A., Zheng, G.R., 1998. Metamorphic core complex in Ganzhuermiao, Inner Mongolia. Acta Geologica Sinica 33, 140–146 (in Chinese with English abstract).
Zhang, H.F., Sun, M., Zhou, X.H., Fan, W.M., Zhai, M.G., Yin, J.F., 2002a. Mesozoic lithosphere destruction beneath the North China Craton: evidence from major, trace element, and Sr–Nd–Pb isotope studies of Fangcheng basalts. Contributions to Mineralogy and Petrolgy 144, 241–253.
Zhang, Y.B., Wu, F.Y., Li, H.M., Lu, X.P., Sun, D.Y., Zhou, H.Y., 2002b. Single grain zircon U–Pb ages of the Huangniling granite in Jilin Province. Acta Petrologica Sinica 18, 475–481 (in Chinese with English abstract).
Zhang, Y.B., Wu, F.Y., Wilde, S.A., Zhai, M.G., Lu, X.P., 2004. Zircon U–Pb ages and tectonic implications of 'Early Paleozoic' granitoids at Yanbian, Jilin Province, northeast China. The Island Arc 13, 484–505.
Zhang, J.H., Ge, W.C., Wu, F.Y., Liu, X.M., 2006a. Mesozoic bimodal volcanic suite in Zhalantun of the Da Hinggan Range and its geological significance: zircon U–Pb age and Hf isotopic constraints. Acta Geologica Sinica 80, 58–69.
Zhang, Y.T., Zhang, L.C., Ying, J.F., Zhou, X.H., 2006b. Geochemistry of Zhalantun dyke swarm in north Da Hinggan Mountain and its geological implication. Acta Petrologica Sinica 22, 2733–2742 (in Chinese with English abstract).
Zhang, Y.B., Sun, S.H., Mao, Q., 2006c. Mesozoic O-type adakitic volcanic rocks and its petrogenesis, paleo-tectonic dynamic and mineralization significance of the eastern side of southern Da Hinggan, China. Acta Petrologica Sinica 22, 2289–2304.
Zhang, H.F., Nakamura, E., Sun, M., Kobayashi, K., Zhang, J., Ying, J.F., Tang, Y.J., Niu, L.F., 2007a. Transformation of subcontinental lithospheric mantle through peridotite-melt reaction: evidence from a highly fertile mantle xenolith from the North China Craton. International Geology Review 49, 658–679.
Zhang, F.Q., Pang, Y.M., Yang, S.F., Dong, C.W., Chen, H.L., Shu, P., 2007b. Geochronology of zircon SHRIMP, geochemistry and its implication of the volcanic rocks from Yingcheng Formation in depression area, north of Songliao Basin. Acta Geologica Sinica 81, 1249–1259 (Chinese Edition).
Zhang, Y.B., Wu, F.Y., Zhai, M.G., Lu, X.P., Zhang, H.F., 2007c. Geochronology and tectonic implications of the Seluohe Group in the northern margin of the North China Craton. International Geology Review 50, 135–153.
Zhang, L.C., Chen, Z.G., Zhou, X.H., Wang, F., Zhang, Y.T., 2007d. Characteristics of deep sources and tectonic-magmatic evolution of the early Cretaceous volcanics in Ganhe area, Da-Hinggan Mountains: constraints of Sr–Nd–Pb–Hf isotopic geochemistries. Acta Petrologica Sinica 23, 2823–2835 (in Chinese with English abstract).
Zhang, J.H., Ge, W.C., Wu, F.Y., Wilde, S.A., Yang, J.H., Liu, X.M., 2008b. Large-scale Early Cretaceous volcanic events in the northern Great Xing'an Range, Northeastern China. Lithos 102, 138–157.
Zhang, L.C., Zhou, X.M., Ying, J.F., Wang, F., Guo, F., Wan, B., Chen, Z.G., 2008c. Geochemistry and Sr–Nd–Pb–Hf isotopes of Early Cretaceous basalts from the Great Xinggan Range, NE China: implications for their origin and mantle source characteristics. Chemical Geology 256, 12–23.
Zhang, F.Q., Chen, H.L., Dong, C.W., Yu, X., Xiao, J., Pang, Y.M., Cao, R.C., Zhu, D.F., 2008a. Evidence for the existence of Precambrian Basement under the northern Songliao basin. Geology of China 35, 421–428 (in Chinese with English abstract).
Zhao, G.L., Yang, G.L., Fu, J.Y., Wang, Z., Fu, J.Y., Yang, Y.Z., 1989. Mesozoic volcanic rocks in central and southern Da Hinggan Ling Range. Beijing Science and Technology Publishing House, 1–260 (in Chinese with English abstract).
Zheng, J.P., O'Reilly, S.Y., Griffin, W.L., Lu, F.X., Zhang, M., 1998. Nature and evolution of Cenozoic lithospheric mantle beneath Shandong Peninsula, Sino-Korean Craton, Eastern China. International Geology Review 40, 471–499.
Zheng, J.P., O'Reilly, S.Y., Griffin, W.L., Lu, F.X., Zhang, M., Pearson, N.J., 2001. Relict refractory mantle beneath the eastern North China block: significance for lithosphere evolution. Lithos 57, 43–66.
Zheng, J.P., Griffin, W.L., O'Reilly, S.Y., Yang, J.S., Li, T.F., Zhang, M., Zhang, R.Y., Liou, J.G., 2006. Mineral chemistry of peridotites from Paleozoic, Mesozoic and Cenozoic lithosphere: constraints on mantle evolution beneath Eastern China. Journal of Petrology 47, 2233–2256.

Zheng, J.P., Griffin, W.L., O'Reilly, S.Y., Yu, C.M., Zhang, H.F., Pearson, N., Zhang, M., 2007. Mechanism and timing of lithospheric modification and replacement beneath the eastern North China Craton: peridotitic xenoliths from the 100 Ma Fuxin basalts and a regional synthesis. Geochimica et Cosmochimica Acta 71, 5203–5225.

Zhou, X.M., 2003. My thinking about granite geneses of South China. Geological Journal of China Universities 9, 556–565 (in Chinese with English abstract).

Zhou, X.M., Li, W.X., 2000. Origin of Late Mesozoic igneous rocks of Southeastern China: implications for lithosphere subduction and underplating of mafic magma. Tectonophysics 326, 269–287.

Zhou, M.F., Zhang, H.F., Robinson, P.T., Malpas, J., 2003. Comments on "Petrology of the Hegenshan ophiolite and its implication for the tectonic evolution of northern China" by T. Nozaka and Y. Liu [Earth Planet. Sci. Lett. 202 (2002) 89–104]. Earth and Planetary Science Letters 217, 207–210.

Zhou, C.Y., Wu, F.Y., Ge, W.C., Sun, D.Y., Rahman, A.A.A., Zhang, J.H., Cheng, R.Y., 2005. Age, geochemistry and petrogenesis of the cumulate gabbro in Tahe, northern Da Hinggan Mountain. Acta Petrologica Sinica 21, 763–775 (in Chinese with English abstract).

Zhou, J.B., Wilde, S.A., Zhang, X.Z., Zhao, G.C., Zheng, C.Q., Wang, Y.J., Zhang, X.H., 2009. The onset of Pacific margin accretion in NE China: evidence from the Heilongjiang high-pressure metamorphic belt. Tectonophysics 478, 230–246.